Molecular characterization and pathogenicity potential of novel hantavirus isolates: Greifswald virus from Germany and Sangassou virus, Africa

Dissertation

zur Erlangung des akademischen Grades
doctor rerum naturalium
(Dr. rer. nat.)

im Fach Biologie

eingereicht an der
Mathematisch-Naturwissenschaftlichen Fakultät I
der Humboldt-Universität zu Berlin

von Dipl. Chem. Elena Popugaeva

Präsident der Humboldt-Universität zu Berlin

Prof. Dr. Jan-Hendrik Olbertz

Dekan der Mathematisch-Naturwissenschaftlichen Fakultät I
Prof. Dr. Andreas Herrmann

Gutachter: 1. Prof. Dr. Detlev H. Krüger

2. Prof. Dr. Heribert Hofer

3. PD Dr. Thorsten Wolff

Tag der mündlichen Prüfung: 16.02.2012

Summary

Hantaviruses are worldwide distributed pathogens which are mainly carried by rodents. When transmitted to humans, they can cause two significant diseases: hemorrhagic fever with renal syndrome (HFRS) or hantavirus cardiopulmonary syndrome (HCPS). Depending on the virus strain, the case fatality rates of hantavirus diseases are ranging from 0.1% up to 50%.

In Europe Dobrava-Belgrade virus (DOBV) is the most life-threatening hantavirus leading to HFRS with case fatality rates of up to 12%. According to its natural hosts, mice of the genus *Apodemus,* DOBV forms distinct phylogenetic lineages. DOBV-Af associated with *A. flavicollis* (Af) causes severe HFRS cases in the Balkan region. DOBV-Aa, found in *A. agrarius* (Aa), is typical for Central Europe and Central European Russia where it causes mild/moderate disease. Moderate to severe HFRS cases in South European Russia have been associated with virus strains of the DOBV-Ap lineage, transmitted by *A. ponticus* (Ap).

In Germany, DOBV is endemic in the northern part of the country. Seroepidemiological studies involving fine serotyping by neutralization assay as well as phylogenetic analyses of patient-associated virus sequences showed that strains of DOBV-Aa lineage are responsible for HFRS cases in this geographical region. However, the causative agent of human disease from Germany was not isolated in cell culture.

Within the current study, we have generated the first cell culture isolate of DOBV from Germany, called Greifswald virus (GRW/Aa), and determined its complete genomic nucleotide sequence. Phylogenetic analyses revealed close clustering of GRW/Aa with sequences derived from Northern German HFRS patients. Consequently, GRW/Aa can be taken as a representative of DOBV strains causing HFRS in Germany. We have demonstrated that in cultivated host cells GRW/Aa exhibits properties similar to pathogenic Hantaan virus; it recognizes β3 integrins and Decay Accelerating Factor (DAF) as cellular entry receptors and induces late expression of innate immunity markers (IFN-β, IFN-λ1, MxA).

Despite hantaviruses being well recognized human pathogens in almost all continents, the first African hantavirus named Sangassou virus (SANGV) has been only very recently isolated in our group. Important to note that SANGV is most closely related to DOBV in molecular phylogenetic analyses. Therefore, it was interesting to investigate if SANGV, a potential human pathogen, displays properties similar to GRW/Aa. Given that an animal model for studying hantavirus-mediated pathogenesis is not available, we used cellular receptor recognition and induction of innate immunity markers as in vitro determinants to

estimate the pathogenic potential of SANGV in comparison to GRW/Aa. We have found that SANGV exclusively recognizes β1 integrins as cellular entry receptors and elicits strong induction of IFN-λ1 in infected cells. Therefore, in cultivated host cells SANGV exhibits functional characteristics distinct from GRW/Aa. Whether these properties contribute to SANGV-mediated pathogenesis in humans needs to be elucidated in future studies.

Keywords: Dobrava-Belgrade virus (DOBV); Sangassou virus (SANGV), cellular receptor; innate immunity.

Zusammenfassung

Hantaviren, deren Hauptreservoir Nager bilden, sind weltweit verbreitete Pathogene. Nach Übertragung auf den Menschen prägen sie vorwiegend zwei Krankheitsbilder: Das hämorrhagische Fieber mit renalem Syndrom (HFRS) oder das Hantavirus-assoziierte cardiopulmonale Syndrom (HCPS). Je nach Virusstamm variiert die Mortalitätsrate zwischen 0,1% und 50%.

Das Dobrava-Belgrad-Virus (DOBV), welches zum HFRS führt, weist eine Mortalitätsrate von bis zu 12% auf und ist somit das lebensbedrohlichste Hantavirus in Europa. Wie ihre natürlichen Wirte, die Mäuse aus dem Genus *Apodemus,* bilden auch die DOBV unterschiedliche phylogenetische Linien. Das aus *A. flavicolis* (Af) isolierte DOBV-Af ist im Balkan verbreitet und führt zu schweren Verläufen des HFRS. Das in *A. agrarius* (Aa) gefundene DOBV-Aa verursacht schwache bis milde HFRS-Erkrankungen in Mitteleuropa und dem zentraleuropäischen Teil Russlands. Moderate bis schwere HFRS-Verläufe im südeuropäischen Teil Russlands wurden mit Viren der DOBV-Ap-Linie in Verbindung gebracht, welche von *A. ponticus* (Ap) übertragen werden.

In Deutschland ist DOBV endemisch im nördlichen Teil des Landes. Epidemiologische Studien, basierend auf der serologischen Feintypisierung mittels Neutralisationstests und phylogenetischen Analysen Patienten-assoziierter Virussequenzen, zeigen, dass Viren der DOBV-Aa-Linie für die HFRS-Fälle in dieser Region verantwortlich sind. Bislang konnte das für die humane Erkrankung in Deutschland verantwortliche Virus noch nicht in Zellkultur isoliert werden.

In der vorliegenden Arbeit wurde das erste Zellkulturisolat eines aus Deutschland stammenden DOBV gewonnen, dessen vollständige Genomsequenz bestimmt und als Greifswald-Virus (GRW/Aa) bezeichnet wurde. In phylogenetischen Analysen bildete GRW/Aa eine gemeinsame Gruppe mit viralen Sequenzen, die aus norddeutschen HFRS-Patienten gewonnen wurden. Folglich kann GRW/Aa als das für HFRS in Deutschland verantwortliche DOBV angesehen werden. Anhand von Wirtszellkulturen konnten wir zeigen, dass GRW/Aa ähnliche Charakteristika aufweist, wie das pathogene Hantaan-Virus; es nutzt β3-Integrine und den *decay accelerating factor* (DAF) als zelluläre Rezeptoren und induziert die späte Expression von Markern der angeborenen Immunantwort (z. B. IFN-β, IFN-λ1, MxA).

Obwohl Hantaviren auf nahezu allen Kontinenten als Humanpathogene bekannt sind, wurde das erste afrikanische Hantavirus (Sangassou-Virus, SANGV) erst kürzlich in unserer Arbeitsgruppe isoliert. Aufgrund der engen phylogenetischen Verwandtschaft zwischen SANGV und GRW/Aa haben wir untersucht, ob das potentiell humanpathogene SANGV ähnliche Eigenschaften wie GRW/Aa aufweist. Aufgrund der Tatsache, dass bislang noch kein Tiermodell für die Untersuchung der Hantaviruspathogenese existiert, haben wir die Rezeptorerkennung und Induktion der Marker der angeborenen Immunantwort zur Abschätzung des humanpathogenen Potentials von SANGV, im Vergleich zu GRW/Aa, verwendet. Wir zeigten, dass SANGV ausschließlich β1-Integrine als Rezeptor nutzt und eine starke IFN-λ1-Antwort in der infizierten Zelle induziert. In der Zellkultur zeigt SANGV somit andere funktionelle Charakteristika als GRW/Aa. Ob diese in Zusammenhang mit einer durch SANGV vermittelten Pathogenese stehen, muss in zukünftigen Studien untersucht werden.

Schlagwörter: Dobrava-Belgrad-Virus (DOBV); Sangassou virus (SANGV), zellulärer Rezeptor, angeborene Immunantwort.

Abbreviations

aa	amino acid(s)	G1	glycoprotein 1
Aa	*Apodemus agrarius*	G2	glycoprotein 2
Af	*Apodemus flavicollis*	HFRS	Hemorrhagic Fever with Renal Syndrome
Ap	*Apodemus ponticus*	HCPS	Hantavirus Cardiopulmonary Syndrome
APS	ammonium persulfate	h	hour(s)
BSA	bovine serum albumin	HTNV	Hantaan virus
BSL	biosafety level	ICTV	International Committee on Taxonomy of Viruses
bp	base pair(s)	HRP	horseradish peroxidase
cDNA	complementary DNA	IFN	interferon
CAR	coxsackie and adenovirus receptor	IRF	IFN regulatory factor
DAF	Decay Accelerating Factor	Ig	immunoglobulin
DNA	deoxyribonucleic acid	ISG	interferon stimulated gene
DOBV	Dobrava-Belgrade virus	JAK	janus protein tyrosine kinase
DMEM	Dulbecco's modified Eagle medium	L-segment	large genome segment
d	day(s)	min	minutes
ds	double stranded	MOI	multiplicity of infection
eIF2a	eukaryotic translation initiation factor 2a	M-segment	medium genome segment
ELISA	enzyme-linked immunosorbent assay	mRNA	messenger RNA
FCS	fetal calf serum	ML	maximum likelihood
FFU	focus forming units	MEM	minimum essential medium
FITC	fluorescein isothiocyanate	N	nucleocapsid
GRW/Aa	Greifswald virus	NC	negative control
nt	nucleotide(s)	NCR	non-coding region
NS	non-structural	UV	ultraviolet
OD	optical density	ucf	ultracentrifuged

ORF	open reading frame	vRNA	viral RNA
PC	positive control	VEGF	vascular endothelial growth factor
PCR	polymerase chain reaction	VEGFR2	VEGF cellular receptor 2
PBS	phosphate buffered saline	WB	Western blot
PSI	plexin–semaphorin–integrin	wt	wild type
PKR	protein kinase R		
PHV	Prospect Hill virus		
pi	post infection		
qPCR	quantative real-time PCR		
RdRp	RNA dependent RNA polymerase		
RGD	arginine-glycine-aspartic acid		
RT-PCR	reverse transcription PCR		
RNA	ribonucleic acid		
SANGV	Sangassou virus		
SD	standard deviation		
SDS	sodium dodecyl sulphate		
S-segment	small genomic segment		
STAT	signal transducer of activation and transcription		
SK	Slovakia		
Slo	Slovenia		
TEMED	Tetramethylethylenediamine		
TNF	tumor necrosis factor		
U	unit(s)		

Table of Content

1 Introduction

1.1 Historical overview

The history of the hantavirus research starts in 1976 when Ho-Wang Lee and co-workers isolated the first hantavirus from striped field mouse (*Apodemus agrarius*). It was named Hantaan virus (HTNV) according to the Hantaan River which flows through the endemic region of Korea [1]. HTNV is an etiological agent of human disease known as hemorrhagic fever with renal syndrome (HFRS) characterized by symptoms such as high fever, chills, headache, generalized myalgia, abdominal and back pain and hemorrhagic manifestations [2]. The term „HFRS“ was adopted by the World Health Organization in 1983 to serve as an unifying name for clinical hantavirus infections in Eurasia [3]. Before, the disease had a multitude of names that brought much confusion concerning its actual distribution and epidemiology. In China the disease was known as epidemic hemorrhagic fever while it was called Korean hemorrhagic fever in Korea. In Scandinavia, western USSR, and Western Europe, the disease was called nephropathia epidemica.

Description of the first clinical cases of human disease with characteristics similar to HFRS have been found in the archives of a hospital in Vladivostok (Far Eastern Siberia, Russia) in 1913 [4]. However, Chinese physicians described the disease more than 1000 years ago. Intensive research on hantaviruses started after the Korean War (1950-1953) when more than 3,000 American soldiers developed the illness of unknown etiology [5].

Isolation of the HFRS agent had been attempted by several groups of investigators since 1952, but successful hantavirus propagation in cell culture was achieved only in 1981 [6]. Although viral antigens and RNA are present in the tissues of most seropositive natural hosts – rodents, the viruses are very often difficult to establish in tissue culture by direct inoculations.

After discovery of the first hantavirus, other viruses genetically related to the Hantaan virus were characterized and classified: Puumala virus (PUUV) from bank voles [7], Seoul virus (SEOV) from urban rats [8] and Dobrava-Belgrade virus (DOBV) from yellow-necked field mouse [9].

First in 1993 Sin Nombre hantavirus (SNV) from deer mouse was identified as a causative agent of a mysterious respiratory illness in the United States with high case fatality rates, today known as hantavirus cardiopulmonary syndrome [10]. Later on several new hantavirus species from the Americas have been described: New York virus (NYV) from white-footed mouse [11] and Andes virus (ANDV) from long-tailed pygmy rice rat [12]. However, the

non-pathogenic Prospect Hill virus (PHV) from meadow vole was already described in 1985 [13].

Lately, the first indigenous African hantavirus, Sangassou virus (SANGV), was found in the African wood mouse from Guinea, West Africa [14]. Meanwhile, two additional hantaviruses were found in Africa – Tanganya virus [15] and Azagny virus [16].

Until recent time, rodents were considered as sole natural hosts for hantaviruses. Thottapalayam virus (TPMV), isolated from an Asian house shrew trapped in India, was for many years considered as a single exception (for the references see [17]). However, several recent studies indicated that multiple other species of shrews from widely separated geographic regions harbor hantaviruses that are far more genetically divergent than hantaviruses carried by rodents. Shrew-borne hantaviruses include Tanganya virus in the Therese's shrew, Azagny virus harbored by the West African pygmy shrew, Camp Ripley virus (RPLV) in the northern short-tailed shrew [18], Cao Bang virus (CBNV) in the Chinese mole shrew [19], Seewis virus (SWSV) in the Eurasian common shrew [20], Ash River virus (ARRV) in the masked shrew [21], Jemez Springs virus (JMSV) in the dusky shrew [21], and Imjin virus (MJNV) in the Ussuri white-toothed shrew [22]. In addition, phylogentically distinct hantaviruses from moles have been identified. Mole-borne hantaviruses include Asama virus (ASAV) in the Japanese shrew mole [23], Oxbow virus (OXBV) in the American shrew mole [24], and Nova virus (NVAV) in the European common mole [25].

1.2 Genome structure and replication

Hantaviruses belong to the *Bunyaviridae* family. Replication takes place in the cytoplasm of infected cells. Their virions are spherical particles with diameters from 90 nm to 100 nm. The virus has a three-segmented RNA genome of negative polarity. The S-segment open reading frame (ORF) encodes a viral nucleocapsid (N-protein). In some viruses, e.g. PUUV and SNV, there is an additional small ORF overlapping with the major open reading frame of the S mRNA which encodes a putative non-structural protein [26]. Hantaviruses have an envelope that is formed by a lipid bilayer and two glycoproteins, G1 and G2. These proteins are cleavage products of a glycoprotein precursor encoded by M-segment ORF. The L-segment ORF encodes a RNA-dependent RNA polymerase (L-protein). The L-protein has been reported to have many functions such as transcriptase, replicase and endonuclease [27]. Viral RNAs are encapsidated by N-protein forming viral ribonucleoprotein complexes (vRNP). A small amount of L-protein is also associated with each vRNP (Figure 1).

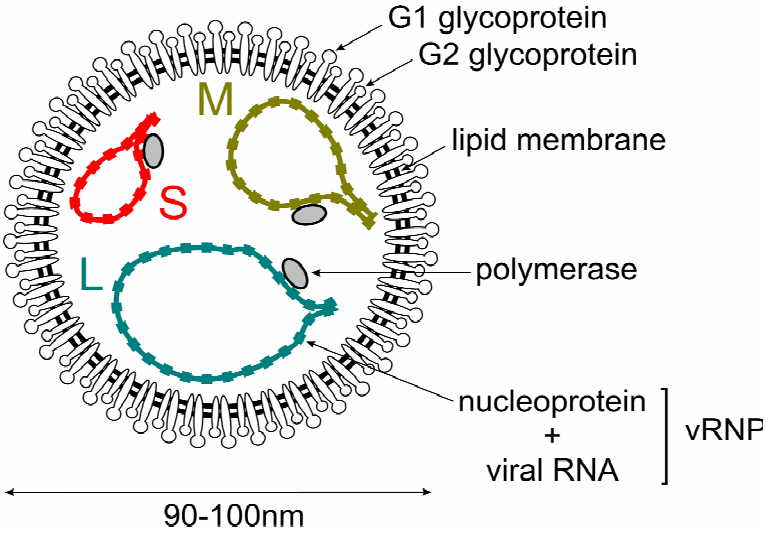

Figure 1: Schematic illustration of a hantavirus particle (adapted from Dr. B. Klempa)

The vRNPs of hantaviruses appear to be circular due to the complementarity and subsequent base pairing of the 5'- and 3'-termini of the vRNAs. The 5'- and 3'-termini of all three segments form panhandle structures. These panhandles are thought to play a role in viral transcription and in the proposed prime-and-realign mechanism of replication [28].

Negative-stranded RNA viruses which replicate either in the cell nucleus (orthomyoxviruses) or in the cell cytoplasm (bunyaviruses) have not evolved capping enzymes, but evolved unique strategies to cap their own mRNA. Hantaviruses get hold of caps from the host cell mRNAs by a novel cap-snatching mechanism [29].

The model of hantavirus transcription of vRNA to mRNA is termed "prime-and-realign". It suggests that the terminal G-residue from the cellular cap primer aligns with the third nucleotide of the hantaviral vRNA (C-residue) to initiate the L-protein transcriptase activity. After synthesis of a few nucleotides, the nascent RNA realigns by slipping backwards three nucleotides on the repeated terminal sequences (AUC(+3)AUC(+6)AUC) of the S-, M-, and L-RNAs. The outcome of the slippage is that the G becomes the first nucleotide of the 5'-extensions. This realignment of the G to the position -1 produces an extra copy of the 3'-end of viral mRNA. However, if the G initiates at position +6, rather than +3, and realigns to position +3, the first two nucleotides of the viral mRNA will be lost, a finding that is commonly observed in sequence studies ([30], Figure 2).

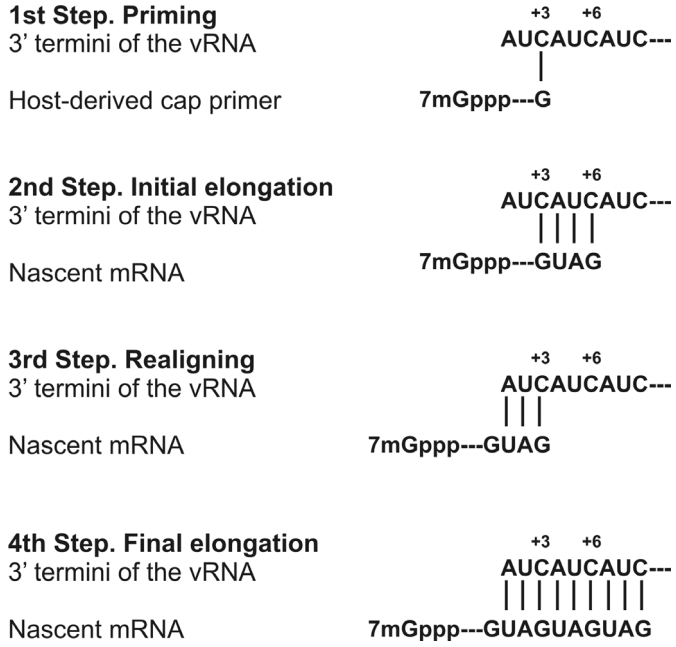

Figure 2: Prime-and-realign model for initiation of hantavirus mRNA synthesis (adapted from [27]**).**

The same prime-and-realign model has been proposed for vRNA and cRNA synthesis during hantavirus replication with a single difference. GTP is used as a primer for initiation of virus replication [28]. The accumulation of N-protein is most likely the signal for switching from primary transcription to replication. Newly synthesized N-protein is required for genome replication [31,32] and therefore mRNA transcription and translation of viral proteins starts before the RNA replication.

1.3 Natural host reservoirs

TPMV was isolated in 1971 from Asian house shrew before the first prototype of hantaviruses – HTNV has been obtained from a rodent. However, TPMV was classified as a hantavirus much later than HTNV. Therefore, for many years murid rodents (order *Rodentia*; family *Muridae*, subfamily *Murinae*; family *Cricetidae,* subfamilies *Arvicolinae*, *Sigmodontinae* and *Neotominae*) were considered as natural hosts of hantaviruses [33], Table 1. However, recently new distinct hantaviruses of currently unknown pathogenic potential have been discovered in insectivorous shrews and moles (for references see chapter 1.1).

Phylogenetic analyses revealed significant congruence (similarity) in genetic co-evolution of hantaviruses with their natural hosts [34]. Therefore, it was believed that hantavirus species are co-evolved with their rodent hosts. It is still thought that hantavirus species are strongly associated with one (or a few closely related) specific rodent species. Although, several studies showed that there might be multiple rodent hosts for particular virus species and multiple viruses can exist in a single host species [33,35].

Table 1: Selected hantavirus species and their natural hosts (adapted from [36,37,23,24])

species	host		abbreviation of virus name
	Murinae-associated	rodents	
Dobrava-Belgrade virus	*Apodemus flavicollis*		DOBV-Af
	Apodemus agrarius		DOBV-Aa
	Apodemus ponticus		DOBV-Ap
Hantaan virus	*Apodemus agrarius*		HTNV
Seoul virus	*Rattus species*		SEOV
Sangassou virus	*Hylomyscus simus*		SANGV
	Arvicolinae-associated		
Puumala virus	*Myodes glareolus*		PUUV
Tula virus	*Microtus arvalis, M. agrestis, M. rossiaemeridionalis*		TULV
Prospect Hill virus	*Microtus pennsylvanicus, M. ochrogaste*r		PHV
	Neotominae-associated		
Sin Nombre virus	*Peromyscus maniculatus*		SNV
New York virus	*P.leucopus Peromyscus leucopus*		NYV
El Moro Canyon virus	*Reithrodontomys megalotis*		ELMCV
Rio Segundo virus	*Reithrodontomys mexicanus*		RIOSV
	Sigmodontinae-associated		
Andes virus	*Oligoryzomys longicaudatus*		ANDV
Maporal virus	*Oligoryzomys fulvescens*		MAPV
Black Creek Canal virus	*Sigmodon hispidus*		BCCV
	Crocidurinae-associated	shrews	
Thottapalayam virus	*Suncus murinus*		TPMV
Tanganya virus	*Crocidura theresae*		TGNV
Azagny virus	*Crocidura obscurior*		AZGV
	Soricinae-associated		
Ash River virus	*Sorex cinereus*		ARRV
Seewis virus	*Sorex araneus*		SWSV
	Talpinae-associated	moles	
Asama virus	*Urotrichus talpoides*		ASAV
Oxbow virus	*Neurotrichus gibbsii*		OXBV
Nova virus	*Talpa europaea*		NVAV

Hantaviruses are maintained by horizontal transmission through close contact (e.g. bites) between natural hosts. In contrast to humans, hantaviruses persistently infect their reservoir hosts, causing life-long infections, mainly without signs of disease. Hantavirus infection in natural hosts is characterized by an acute phase of peak viremia, viral shedding, and virus replication in target tissues, followed by a persistent phase of reduced, cyclical virus replication despite the presence of high antibody titers [38]. Humans are dead-end hosts, spill-over infection to them results in the hantavirus disease, characterized in severe cases by renal or lung failure.

1.4 Evolution of hantaviruses

The separation of hantaviruses into clades that parallel the molecular phylogeny of rodents in the *Murinae*, *Arvicolinae*, *Neotominae*, and *Sigmodontinae* subfamilies has suggested that hantaviruses have co-evolved with their reservoir rodent hosts [34,39] (Figure 3). Recently, this idea has been actively challenged on the basis of the disjunction between the evolutionary rates of the host and virus species [40,41]. Host switching and local species-specific adaptation instead of co-divergence have been speculated to account for the similarities between the host and virus phylogenies.

Obviously, host switching (virus shifting to a new host) have occurred during the evolution of the rodent-borne hantavirus (Topografov virus in Siberian lemmings (*Lemmus sibiricus*) is an often cited example) as well as during the evolution of the insectivore-borne hantaviruses (for references see review [42]). The evolution of hantaviruses has been also influenced by reassortment and recombination events [43]. In the Old and New World, reassortment of hantaviruses have been reported to occur in nature within and between virus lineages, and even between different viruses [44-46].

Recent emergence of hantaviruses isolated from shrews and moles of multiple species suggests that evolutionary history of hantaviruses is even more complex than it was expected. For example, full-genome analysis of Thottapalayam virus (TPMV), a hantavirus isolated from a shrew more than 40 years ago, shows an early evolutionary divergence from rodent-associated hantaviruses [47,48]. Moreover, the collective data including other insectivores-borne hantaviruses suggest that ancestral shrews or moles rather than rodents may have served as the early hosts of primordial hantaviruses [25].

Since the sequence database of hantaviruses from shrews, moles, and other insectivores remains incomplete, it is too early to conclude that recent host switching events coupled with subsequent divergence are solely responsible for the similarities between the phylogenies of hantaviruses and their mammalian reservoir hosts. The issue is not whether the evolution of

hantaviruses is a direct consequence of either host switching or co-phylogeny. Rather, both mechanisms apparently influenced the evolution of hantaviruses. Therefore, when viewed within the context of molecular phylogeny and zoogeography, the close association between distinct hantavirus clades and specific subfamilies of rodents, shrews, and moles is likely the result of alternating and periodic co-divergence through deep evolutionary time [25].

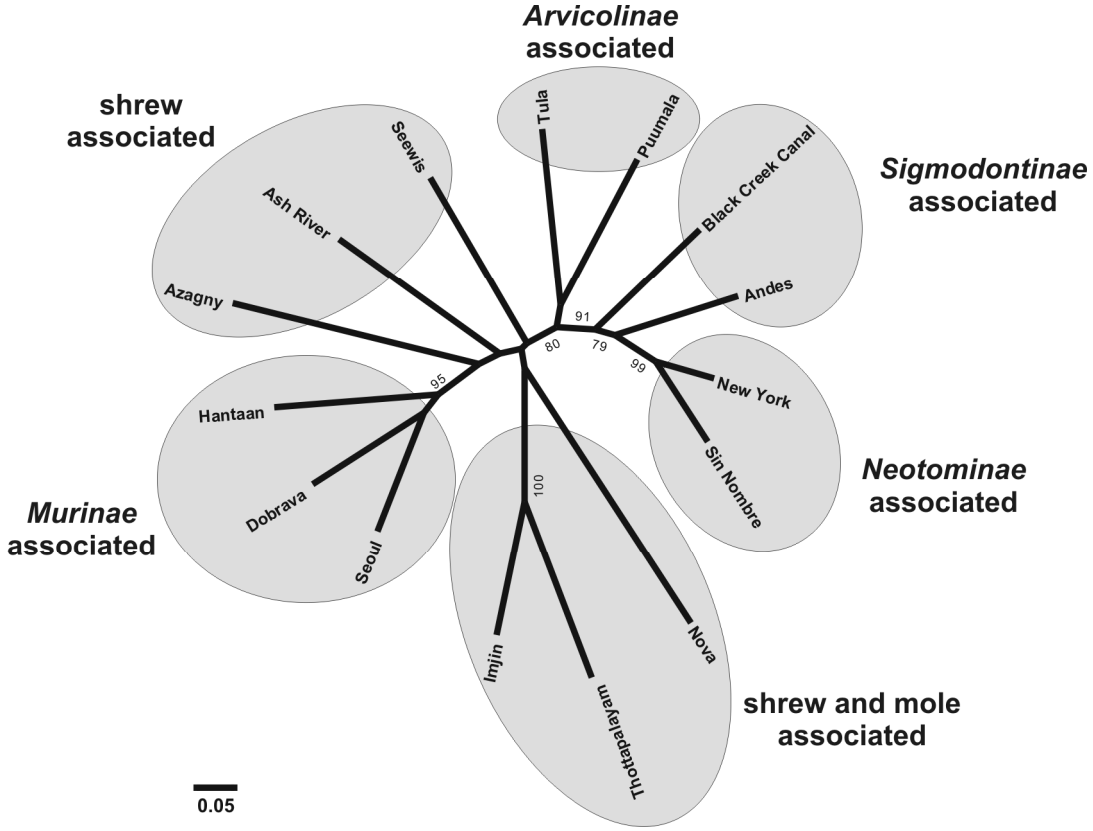

Figure 3: Phylogenetic relationship between selected hantavirus representatives associated with rodents (*Murinae, Arvicolinae, Sigmodontinae* and *Neotominae subfamilies*), shrew and moles. The Maximum likelihood phylogenetic tree (Tamura Nei evolutionary model) is based on partial S-segment nucleotide (418 nucleotides) sequences, calculated with MEGA5.

1.5 The human diseases: Hemorrhagic Fever with Renal Syndrome (HFRS) and Hantavirus Cardiopulmonary Syndrome (HCPS)

Hantaviruses are transmitted to humans through the inhalation of contaminated aerosols from natural hosts excreta and saliva. Both HFRS and HCPS are associated with acute thrombocytopenia and changes in vascular permeability and both syndromes can include renal and pulmonary manifestations. Nevertheless, Old world hantaviruses tend to cause renal dysfunction and the disease is called HFRS while New World hantaviruses are more associated with cardiopulmonary failure (HCPS). Therefore, the latter illness is named HCPS (Table 2).

The incubation time of the disease can take up to 6 weeks. In the very early phase of illness both HFRS and HCPS patients develop influenza-like symptoms, such as fever, chills, general

malaise, headache, abdominal/back pain, and nausea. In the next phases hypotension occurs and a cardiogenic shock can lead to death. In addition, renal or lung failure are also common reasons for a fatal outcome. The appearance of a diuretic phase is usually a good sign of patient recovery. Thereafter, convalescence phase starts and can last up to several weeks [37].

Table 2: Selection of important hantaviruses causing Hemorrhagic Fever with Renal Syndrome (HFRS) and Hantavirus Cardiopulmonary Syndrome (HCPS) in humans

Hantaviruses	Geographical distribution	Disease	Case fatality rates [%]
Old World			
HTNV	Asia	HFRS	10-15
SEOV	Asia	HFRS	<1
PUUV	Europe	HFRS	0.1-0.4
DOBV-Af	Europe	HFRS	up to 12
DOBV-Aa	Europe	HFRS	0.4-0.9
DOBV-Ap	Europe	HFRS	up to 10
New world			
SNV	Americas	HCPS	30-50
ANDV	Americas	HCPS	30-50
NYV	Americas	HCPS	?

1.6 Cellular receptors utilized by hantaviruses during the entry to the target cell

Endothelial cells and platelets are main targets during hantavirus infection. Therefore, it is believed that pathogenesis in humans is dependent on the damage of those cells [49]. Integrins are cellular surface molecules commonly utilized by many non-enveloped and enveloped viruses, including hantaviruses, as receptors for attachment and/or cell entry [50]. They are expressed in many tissues including endothelial cells and platelets [51]. Interestingly for hantavirus research, integrins play a central role in regulating platelet activation and maintaining capillary integrity [49]. The usage of ß3 versus ß1 integrins as receptors for cell entry by hantaviruses seems to be one of the important pathogenicity determinants. It has been shown that ß3 integrin is used predominantly by pathogenic HTNV, SEOV, PUUV, SNV, NYV, ANDV hantaviruses while ß1 integrin is preferentially utilized by non-pathogenic PHV and TULV [49,52-54].

Although, endothelial cells are central targets for hantavirus infection; the main route of virus transmission to humans is the inhalation of contaminated aerosols. Consequently, at the very early stage of infection, the virus attacks the lung epithelium which is a polarized monolayer, meaning that it has apical and basolateral surfaces, connected with each other through tight

junctions. Therefore, the expression of a certain protein is restricted to apical or basolateral localization. Interestingly, ß3 integrins are expressed on basolateral surface of polarized cells; however pathogenic HTNV and PUUV can infect polarized epithelium and endothelium from the apical site, where those receptors are inaccessible. This indicates that hantavirus infection requires an additional target molecule. Recently it has been demonstrated that pathogenic HTNV and PUUV utilize also Decay Accelerating Factor (DAF) [55] during the cell entry process. DAF is a complement factor and is a promising candidate for being an additional receptor for hantaviruses since it is exclusively expressed on the apical site of many polarized cells. Moreover, it has been shown for coxsackievirus that its attachment to the DAF receptor initiates a signaling cascade, leading to the cytoskeletal rearrangements and opening of the tight junctions that facilitate the transport of the viral particle to coxsackie- and adenovirus receptor (CAR). Therefore, it was speculated that hantaviruses can use DAF-mediated signaling to overcome the tight junction barrier in similar way as coxsackievirus does [55].

Another glycoprotein gC1qR/p32 (also called p33 or HABP-1) has been reported to be recognized by HTNV [56]. It is a protein which was initially shown to bind a complement protein C1q. gC1qR/p32 is expressed in many cell types including endothelial cells and platelets. Although, gC1qR/p32 has no trans-membrane domain, it is thought to locate on the cell surface through interactions with other membrane-bound proteins or components. For instance, it has been suggested that association of gC1qR/p32 with ß1 integrin is involved in C1q-mediated endothelial cell adhesion and spreading processes [57]. Furthermore, gC1qR/p32 protein has been shown to interact with viral protein of such viruses as hepatitis C virus, herpes simplex virus type I, rubella virus, adenovirus and others. Since gC1qR/p32 interacts with complement system, it has been speculated that HTNV-mediated recognition of gC1qR/p32 could be involved in dysregulation of the complement pathway. However, how the gC1qR/p32 is implicated in the pathogenesis of HFRS remains to be answered [56].

1.6.1 Permeability changes in endothelial cells caused by pathogenic hantaviruses

Thrombocytopenia is a hallmark of HFRS and HCPS and is one of the prerequisites for hemorrhages in patients suffering from both hantavirus diseases. This indicates that platelets and endothelial cells have to be damaged during hantavirus mediated pathogenesis. In order to maintain a defensive mechanism, endothelial cells migrate on extracellular matrix proteins and therefore support vascular integrity. Such migration is directed by specific integrin-ligand interactions. Ligand binding to integrins results in cytoskeleton rearrangements and is required for cell migration. It has been shown that pathogenic HTNV, NYV, and SEOV inhibited the ability of endothelial cells to migrate on the ß3 integrin ligand - vitronectin, but

had no affect on endothelial cell migration on ß1 integrin ligands - collagen and fibronectin [53]. Given that ß3 integrins, rather than ß1 integrins, have an important role in vascular permeability; the use of ß3 integrins by pathogenic hantaviruses could clarify why infection by these strains results in severe disease. It has been observed that ß3 integrin has two conformations – active (extended) and inactive (bent). It has been shown that hantaviruses can bind to the plexin–semaphorin–integrin (PSI) domain, which is accessible at the apex of the inactive integrin. The binding of hantaviruses to the inactive form of ß3 integrin explains how pathogenic hantaviruses abrogate ß3 integrin-mediated endothelial cell migration, which in turn could lead to the vascular permeability and cause hemorrhages [58].

There is another approach used by hantaviruses in order to dysregulate endothelial cell barrier functions. Hantaviruses enhance endothelial cell permeability in response to the vascular endothelial growth factor (VEGF). VEGF has been reported to cause localized tissue edema and is recognized by the cellular receptor named VEGF receptor 2 (VEGFR2). ß3 integrins have been noted to alter VEGFR2-directed endothelial cell permeability. Therefore, it has been suggested that hantavirus interactions with inactive ß3 integrins has the potential to disrupt VEGFR2-β3 integrin complexes and result in endothelial cells which are hyper-permeabilised. Vascular endothelial (VE)-cadherin is a protein which builds adherence junctions and plays a role in functioning of the endothelial cell barrier (Figure 4). It has been noted that activation of VEGFR2 directs VE-cadherin phosphorylation, dissociation and therefore endothelial cell permeabilisation. In confirmatory assays it was shown that endothelial cells infected with pathogenic HTNV and ANDV increase the dissociation of VE-cadherin [59].

In addition, clinical data demonstrated that platelets from HFRS patients are defective in activation [60], and this explains the thrombocytopenia in hantavirus infected patients. This observation is in agreement with the idea that pathogenic hantaviruses bind the inactive form of ß3 integrin on platelet and on the endothelial cell surface, leading to their altered adherence. In summary, hantavirus mediated dysregulation of ß3 integrin functions may contribute to endothelial cell responses that permeabilise the vasculature [59].

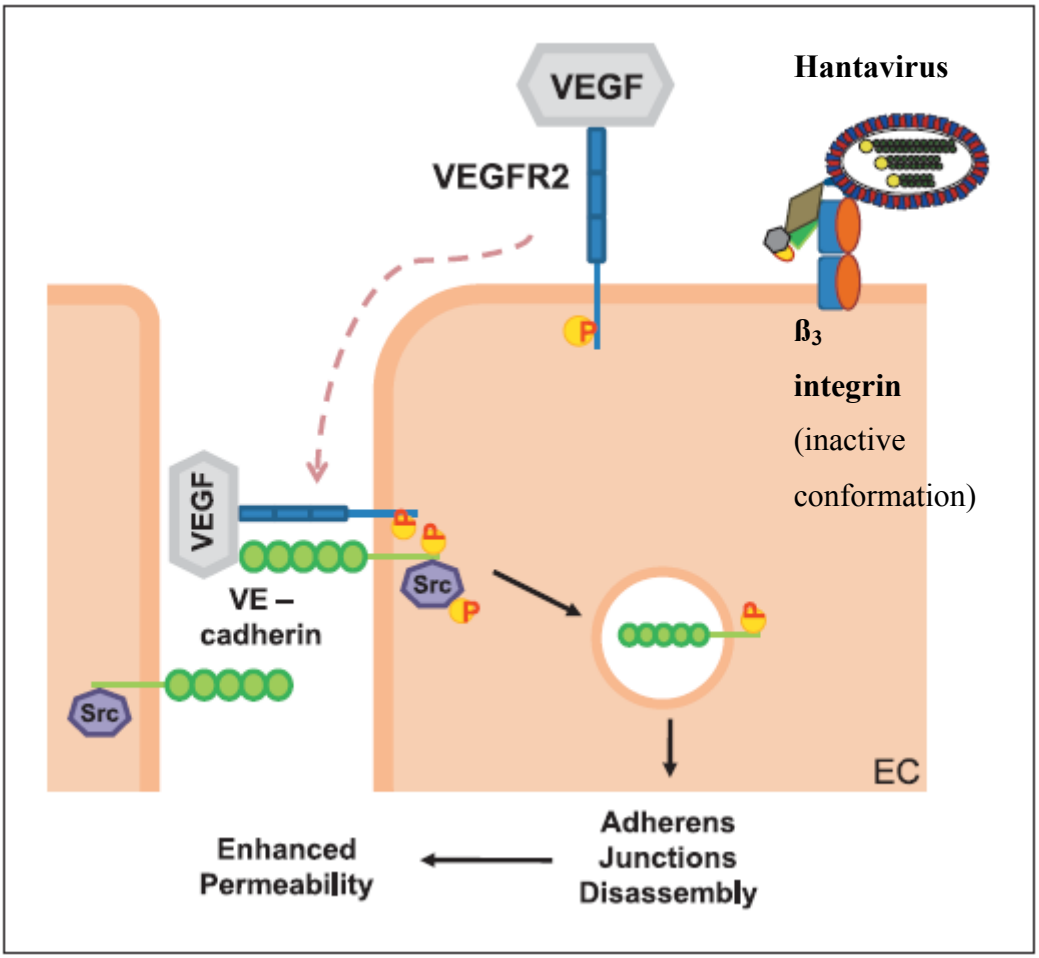

Figure 4: Schematic representation of hantavirus binding to the inactive form of β_3 integrin resulting in enhanced VEGF directed VE-cadherin internalisation, adherens junction disassembly and endothelial cell permeability. EC, endothelial cells. VEGF, vascular endothelial growth factor. VEGFR2, cellular receptor recognising VEGF. VE-cadherin, vascular endothelial protein. Src, kinase that phosphorylates intracellular domain of VE-cadherin (adapted from [59]).

1.7 Hantaviruses and induction of innate immunity

1.7.1 Interferons and their biological activities

Interferons (IFNs) are key players in regulation of innate antiviral responses. There are three types of IFNs (type I, II, and III) which are differentiated accordingly to the structure, receptor usage and biological activity. Type I IFNs form the most abundant family and induce a potent antiviral state in a wide variety of cells, they include 13 types of IFN-α genes and one single gene each of IFN-ß, IFN-κ, IFN-ω, and IFN-ε in humans. There is only one representative of type II IFNs – the IFN-γ gene. It plays a main role in mediating of adaptive immune responses and developing of host protection against pathogenic microorganisms such as bacteria. Interestingly, IFN-γ can amplify the induction of antiviral activity in the presence of IFN-α and IFN-ß, indicating that type I and II IFNs can work together to protect the host

from invading organisms. In 2003, the third family of IFNs (type III) has been discovered which includes three members, IFN-λ1, -λ2, -λ3. Based on their biological activities, type III IFNs are very similar to type I IFNs, however, it has been shown that type III IFNs recognize a different receptor and the expression of type III IFN receptor is restricted to certain cell types.

Although type III IFNs do not recognize receptor utilized by type I IFNs, signaling through either type I or type III receptor leads to the activation of the same Jak-STAT signal transduction cascade (Figure 5).

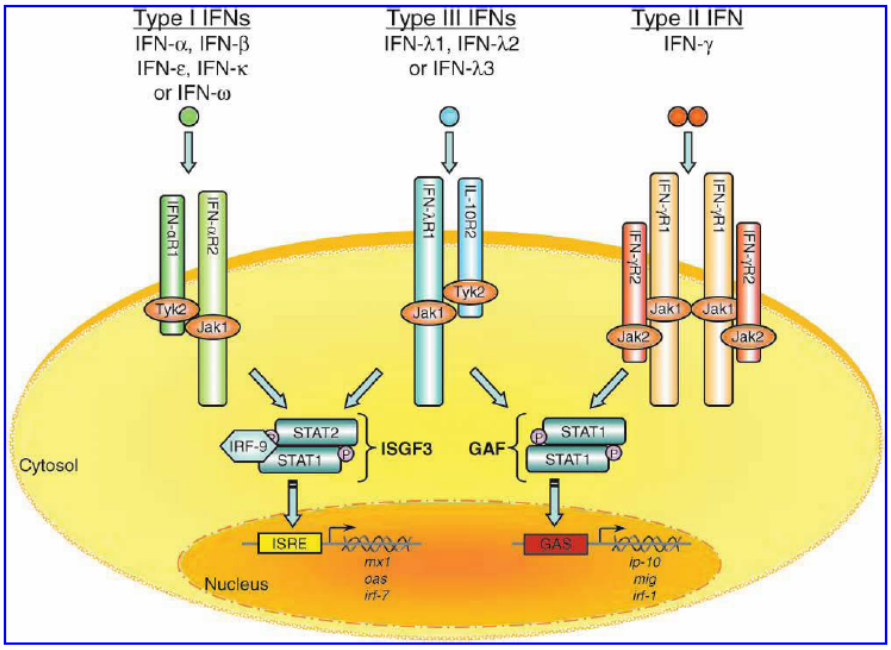

Figure 5: A model of IFN receptor signaling pathway. Type I, II and III IFNs bind to distinct receptor complexes on the cell surface. Signal transduction cascades activated by binding of IFNs to their cognate receptors activate expression of many IFN-stimulated genes (ISGs). The proteins encoded by these genes in turn mediate the antiviral activity of the IFNs, in particular the type I and III IFNs. The recognition of type I or III IFNs by their receptors induces a signaling cascade that results in the activation of STAT1 and STAT2 which together with IRF-9 form ISGF3 transcription factor complexes. The newly formed ISGF3 complexes then translocate from the cytosol to the nucleus where they bind to IFN-stimulated response element (ISRE) in the promoter of ISGs such as IRF7, Mx and OAS genes. (adapted from [61]).

1.7.2 Induction of type I IFNs by hantaviruses

Upon the recognition of the invading virus, the host cell starts to mount antiviral responses, leading to the activation of type I IFNs followed by induced production of ISGs. A strong innate immune response is a very undesirable process for virus replication and its survival in the infected hosts. Therefore, many viruses have developed mechanisms to avoid the host's pathogen-mediated recognition [62,63].

Differential cellular interferon response to pathogenic versus non-pathogenic hantaviruses has been assessed by several research groups. However, the link between the pathogenicity and

ability of certain viruses to induce or counteract expression of IFNs has not been elucidated so far.

There is a study showing that pathogenic HTNV clearly induced the production of IFN-ß, whereas expression of this cytokine was barely detectable in the supernatant or in extracts from cells infected with non-pathogenic TULV [64]. Another study applied Affymetrix DNA array to investigate cellular responses after hantavirus infection in order to differenciate pathogenic SNV hantavirus from non-pathogenic PHV. Authors did not observe significant differences in expression of number of IFN-activated genes in endothelial cells after 4 hours post infection. However, after 12 hours post infection they observed an up-regulation of a small group of genes (anti-viral factors, transcription factors, kinases, structural proteins, receptors, growth factors and chemokines) by PHV in comparison to SNV [65].

Geimonen and Alff observed major differences in IFN-specific transcriptional responses between pathogenic NYV, HTNV and non-pathogenic PHV hantaviruses at 1 day post infection [66,67]. Therefore, the authors suggest that hantavirus pathogenesis may in part be determined by viral regulation of cellular interferon responses. PHV but not pathogenic ANDV, was found to induce a robust IFN-β response early after infection (12 to 24 hours post infection) of primary lung endothelial cells [68]. This finding was confirmed by the observation that PHV but not ANDV activates IFN regulatory factor 3 (IRF-3), which leads to the phosphorylation of IRF-3 and its translocation to the nucleus. In the nucleus IRF-3 stimulates transcription of IFN-β mRNAs. In addition, the level of STAT 1/2 phosphorylation was much lower in cells infected with ANDV [68]. However, Spiropoulou et al found that both ANDV and PHV can down regulate IFN-stimulated phosphorylation of STAT 1/2.

1.7.3 Induction of antiviral MxA gene / protein

A readout marker for IFN bioactivity which has been often used in characterization of hantaviruses is the antiviral MxA protein [64,69-72]. The MxA protein belongs to the superfamily of dimanin-like GTPases and is involved in mediation of antiviral immune response against many viruses [73]. Moreover, it has been shown that over-expression of MxA protein in cell culture can block hantavirus replication [74,75]. An interesting observation has been published recently, demonstrating that established cell lines, such as A549 and HUH7, mount strong MxA response when infected with PHV in comparison to HTNV [71]. Another study observed the strong induction of type III IFNs (IFN- λ1/2) in response to HTNV infection of A549 cells. The induction of IFN- λ1 preceded the induction of MxA and type I IFNs [76]. Since MxA gene expression is regulated only by type I and III IFNs [77], the authors suggested that MxA is induced by type III IFNs in A549 cells exposed

to HTNV. Furthermore, the presence of type III IFNs was detected by ELISA on days 12, 15 and 18 after infection of Vero E6 with PHV, SNV and ANDV, respectively [78]. Vero E6 cells are commonly used by researchers to prepare hantavirus stocks. Presence of active type III IFNs in virus stocks could impair all earlier observed MxA induction patterns in infected cells. Therefore, more investigations are needed to elucidate the influence of newly described type III IFNs in hantavirus-mediated pathogenesis.

1.7.4 The role of protein kinase R in innate immunity and its induction by hantaviruses

IFN inducible protein kinase R (PKR) is one of the four mammalian serine-threonine kinases (the three others being HRI, GCN2 and PERK) that phosphorylates the eIF2a translation initiation factor, in response to stress signals, mainly as a result of viral infections [79]. eIF2a phosphorylation results in the shutdown of translation of both cellular and viral mRNAs - an efficient way to inhibit virus replication. PKR is constitutively expressed at endogenous level in cells, and its activity is regulated by an auto-inhibitory effect of its own N-terminus.

The PKR is activated in response to dsRNA - an intermediate product of viral replication (Figure 6), however, dsRNA is not the sole substrate for PKR. It can be activated by heparin and caspases. It has been shown that heparin binds to the PKR domains and prevents intradomain interactions that in turn lead to the activation of PKR. Caspases are reported to activate PKR through the cleavage of the inhibitory N-terminus from the kinase. In addition, PKR has been observed to mediate indirect phosphorylation and ubiqutination of IκB which leads to the activation of NF-κB pathway ([80], Figure 6). PKR is also activated in response to stress stimuli. Protein activator of the IFN-inducible protein kinase (PACT) has been reported to contribute to PKR-mediated response to stress. Involvement of PACT in PKR-maintained regulation of such transcription factors as NF-κB, STAT-1/3, IRF-1 has been observed [80]. However, PKR-dependent activation of such transcription factors is independent of eIF2a phosphorylation.

Moreover, PKR can function to control cell growth, cell differentiation and can induce apoptosis [79]. Its activity can be controlled by the action of several oncogenes [81].

Viruses have evolved specific mechanisms to prevent the development of an antiviral state by inhibiting key components of the PKR signaling pathway. Several viral proteins antagonists of PKR have been identified, many of which are RNA-binding proteins. For example, non structural proteins (NSs) of Influenza B virus [82] as well as E3L protein from Vaccinia virus were found to inhibit host PKR activity through direct interaction. Hepatitis C virus NS5A, Herpes simplex 1 US11, and Kaposi's sarcoma vIRF-2 proteins also interact with PKR and

inhibit its activity [79]. Some viruses including human cytomegalovirus or mouse cytomegalovirus alter PKR subcellular localization, while others direct PKR to degradation like Rift valley fever virus NSs protein [83].

Despite the fact that PKR plays an important role in the pathogenesis of many different viruses, there are only two publications which tried to evaluate the interactions between hantaviruses and PKR. In the first study, DNA microarray technology was used to monitor changes in mRNA levels after HTNV infection of A549 cells. It was reported that PKR was not involved in antiviral activity during HTNV infection [69]. In the second study, a weak increase in PKR gene expression after PHV infection of endothelial cells was observed [65].

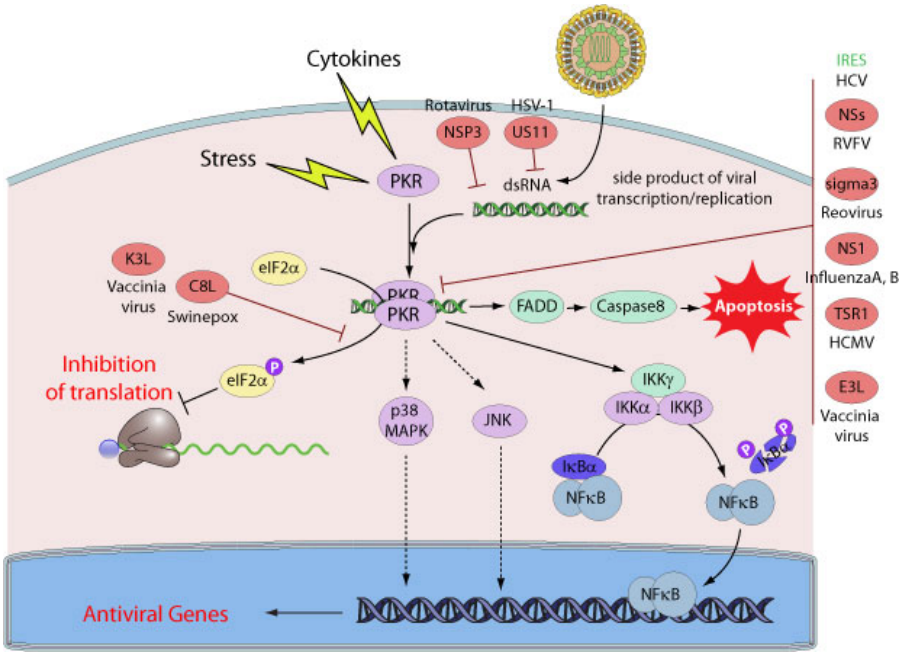

Figure 6: Virus-mediated inhibition of PKR activity
(adapted from http://viralzone.expasy.org/all_by_protein/554.html).

1.8 Hantaviruses in Germany

In Germany hantaviruses cause a rather mild form of HFRS with case fatality rates of up to 0.4% [37]. PUUV is the causative agent for the majority of clinical cases in Germany [84], however DOBV and Tula virus (TULV) are also circulating. The numbers of hantavirus infections of humans in Germany are growing in 2-3 year cycles. For example in 2005, 448 clinical cases were documented; however already in 2007, a major increase (1,687 cases per year) in hantavirus-caused human infections has been registered [84], while in 2010, 2,017 hantavirus infections were reported (data taken from Robert Koch-Institut: SurvStat, http://www3.rki.de/SurvStat). Increased clinical cases of hantavirus infections in Germany are usually associated with increased numbers of bank voles, transmitting the causative agent of disease – PUUV [85]. Intriguingly, a high number of infections in previous years has been observed in urban environments too. This finding could be explained by hypotheses describing bank voles moving close to human habitats due to an exceptionally cold and snowy winter [86]. The difference in reported clinical cases between certain years could be associated with fluctuations in population size of bank voles and the proportion of infected animals. As a consequence, local prevalence and transmission rates can be affected by local age structures, sex ratios and proportion of reproductive voles [85]. Interestingly, the bank vole is distributed through whole Germany; however the majority of PUUV human infections is reported from endemic regions: Baden-Wuerttemberg, Bavaria, North Rhine Westphalia, Lower Saxony [87]. The first PUUV isolate has been generated in the early 80s [7].

The second hantavirus causing human infections in Germany is DOBV. The first case of human infection with DOBV in Germany has been published in 1998 [88]. DOBV-caused HFRS cases are less prevalent then PUUV infections. The distribution of infections with the DOBV seems to be limited to the north-eastern part of Germany (Mecklenburg Western-Pomerania, Brandenburg, Saxony, Saxony-Anhalt), due to the limitation of the geographical distribution of the *Apodemus* mouse as the natural reservoir host of DOBV [89] (Figure 7). There is a study presenting the molecular evidence of *Apodemus agrarius* being a natural host of DOBV in Germany [35].

Another PUUV-related virus – TULV –is considered nowadays as a non-pathogenic hantavirus, however, a single case report, describing possible human infection with TULV has been published [90].

Figure 7: Geographical distribution of hantavirus natural hosts in Germany.

1.9 Dobrava-Belgrade hantavirus (DOBV)

In Europe DOBV is the most life-threatening hantavirus leading to HFRS with case fatality rates of up to 12 % [91,92]. According to the natural hosts, mice of the genus *Apodemus,* DOBV forms distinct phylogenetic lineages. DOBV-Af, represented by the original Dobrava isolate from Slovenia (Slo/Af), associated with *A. flavicollis* (Af), causes severe HFRS cases in the Balkan region. In *A. agrarius* (Aa) two lineages of hantavirus were found. DOBV-Aa, represented by the cell culture isolates SK/Aa from Slovakia and Lipetsk/Aa from Russia, is typical for Central Europe and Central European Russia [93,94], where it causes mild/moderate disease. DOBV-like Saaremaa virus (SAAV) represented by cell culture isolate SAA/160V, present in North-East Europe is not conclusively associated with clinical cases [95]. Very recently, moderate to severe HFRS cases in South European Russia have been associated with the DOBV-Ap lineage, represented by Sochi virus (Sochi/Ap), transmitted by *A. ponticus* (Ap) [94] and an isolate obtained from a fatal human HFRS case (Sochi/hu) [96].

Since natural hosts of DOBV-Af and DOBV-Aa are distributed in the same geographical regions, some interactions between host species could occur. It means that DOBV lineages could undergo the genetic interaction between each other. Molecular phylogenetic analyses indicated possible recombination in DOBV evolution, meaning that DOBV-Af and DOBV-Aa could have interacted with each other in vivo [43].

Photo adapted from Dr. B. Klempa | Photo adapted from Dr. B. Klempa | Photo adapted from Prof. E. Tkachenko

Figure 8: Natural hosts of DOBV. Yellow-necked field mouse, *Apodemus flavicollis*, carrier of DOBV-Af (left); striped field mouse *A. agrarius*, carrier of DOBV-Aa and SAAV (middle); caucasian forest mouse, *A. ponticus*, carrier of DOBV-Ap (right).

Very recently multiple spill-over infections of *A. flavicollis* animals by DOBV-Aa lineage have been reported in Germany [35]. Moreover, single DOBV-Af spill-over infections of *A. sylvanticus* and *Mus musculus* have been reported previously [97]. Virus spill-over infections are good prerequisites for the co-infection of the same animal with different viruses and genetic reassortment between them [98]. In vitro studies, including simultaneous infection of Vero E6 cells with representatives of the DOBV-Aa and DOBV-Af lineages (virus isolates SK/Aa and Slo/Af, respectively), have confirmed reassortment events between two distinct DOBV lineages [72].

It is interesting to note that the different members of the DOBV species exert HFRS of different severity. Most severe human clinical cases were observed in Balkan regions where DOBV-Af infections occur. The case fatality rates were reported to be up to 12%. Whereas clinical manifestations of DOBV-Ap infections of humans in the Sochi region (European Russia) are rather moderate to sever with case fatality rates more than 6%. However, DOBV-Aa have been observed to cause rather mild to moderate courses of HFRS reaching case fatality rates in range from 0.4% to 0.9%. Nevertheless, severe cases of HFRS with renal failure complicated by lung impairment have been observed in Germany [99,98].

Seroepidemiological studies involving fine serotyping by neutralization assay and phylogenetic analysis of patient-associated virus sequences indicated that the DOBV-Aa lineage is responsible for HFRS cases in Northern Germany [100]. Despite of the knowledge that the DOBV is circulating in Germany and causing human disease [100,101,99], the cell culture isolate of the virus could not be generated so far.

1.10 Sangassou virus, the first indigenous hantavirus from Africa

Although hantaviruses are world-wide distributed pathogens, there was only little evidence of hantavirus presence in Africa. There were seroepidemiological reports showing that prevalence of hantavirus antibodies in human populations from different African countries is

in the range from 1.4% to 6.15% [102,103]. Both studies investigated antibodies reacting with HTNV antigen, although *Apodemus agrarius*, the natural host of HTNV, is not found in Africa.

In 2006, the first African hantavirus has been molecularly detected in an African wood mouse (*Hylomyscus simus*) in Guinea. The virus was named Sangassou (SANGV), after the village where the positive animal had been trapped [14]. Phylogenetic analyses based on partial S-, M-, and L-segments revealed that SANGV is a novel hantavirus. First of all, SANGV sequences are significantly divergent (≈ 15%) from other hantavirus species. Second, although SANGV is the most closely related to DOBV, it forms a distinct clade in a Maximum likelihood phylogenetic tree (Figure 9). Third, SANGV was found in a rodent species previously not recognized as a natural host of hantaviruses.

A recent seroepidemiology study based on the combination of screening and confirmatory assays (ELISA, immunoblot, immunofluorescence assay, focus reduction neutralization test) showed the presence of hantavirus-specific neutralizing antibodies in Guinean patients with fever of unknown origin (4.4% seropositive) [104]. In contrast, prevalence of hantavirus antibodies in the whole human population from Forest Guinea was found to be 1.2%. In addition, a serum sample obtained from a patient during the acute phase of illness showed titers of IgM against SANGV that were 4-fold higher than those against PUUV. These data suggest that SANGV (or other related African viruses) might be pathogenic for humans. However, the final evidence of SANGV vRNA being present in human specimens has not been obtained yet.

The second hantavirus from Africa– Tanganya virus (TGNV) was detected in the Therese's shrew (*Crocidura theresae*) [15]. TGNV exhibits low sequence similarity to the rodent derived hantaviruses (below 78%) and showed the lowest similarity to the first described shrew-borne hantavirus - TPMV (below 48% on nucleotide level). Phylogenetic analysis based on partial S-segment sequences revealed that TGNV does not cluster with rodent borne hantaviruses and does not join shrew borne TPMV as well. Nevertheless, evolutionary trees supported the idea that shrew rather than rodent is a natural host for TGNV [15]. Therefore, it is very surprising that TGNV did not form a monophyletic group with TPMV (Figure 9).

Very recently the third hantavirus from Africa, designated Azagny virus (AZGV) was found in the West African pygmy shrew (*Crocidura obscurior*) [16]. Sequence and phylogenetic analyses of the S-, M- and L-segments indicated that AZGV shares a common ancestry with TGNV and is also evolutionarily distant from TPMV. However, to further speculate on

relations of TGNV and AZGV to other shrew-borne hantaviruses more sequence data and epizootiologic studies are necessary.

Taken into account that both TGNV and AZGV exhibit low sequence similarities with rodent-borne hantaviruses, one could expect these viruses being serologically distinct from other hantaviruses. Therefore, human infections by TGNV and AZGV might be missed when using antibody detection assays based on antigens from conventional rodent-borne hantaviruses.

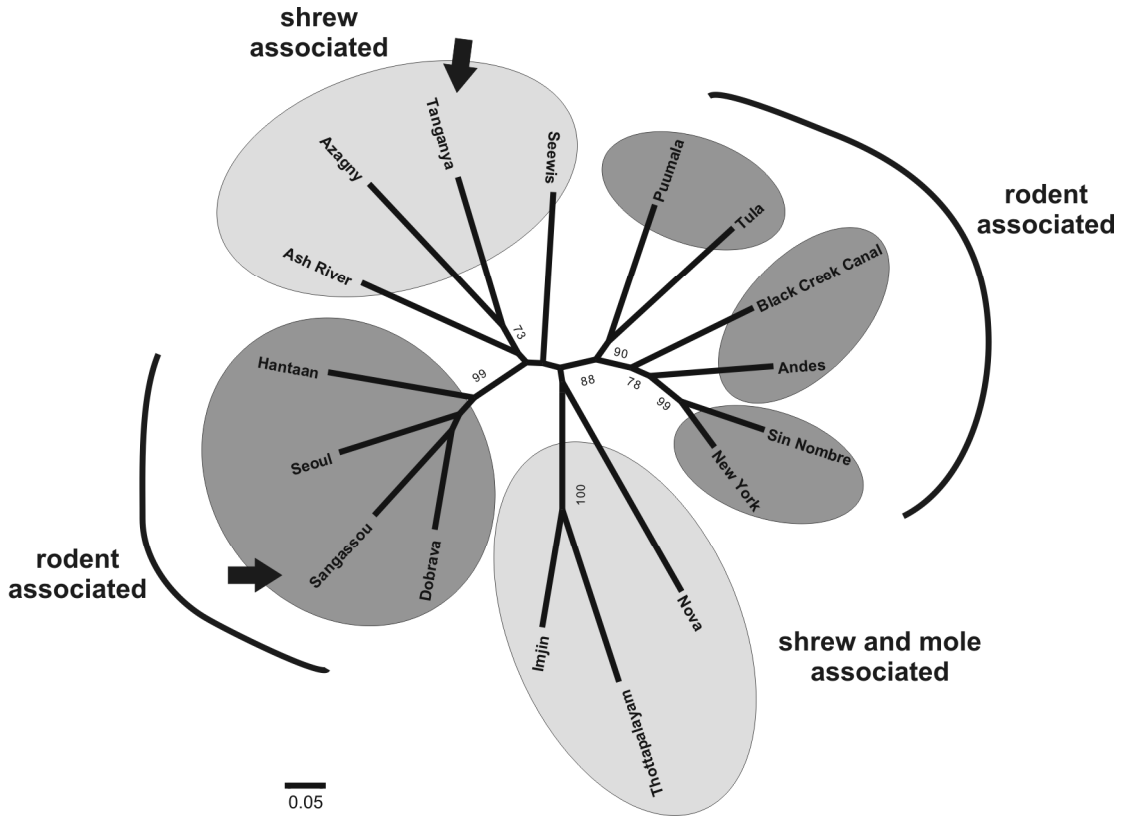

Figure 9: Phylogenetic placement of Sangassou and Tanganya (indicated with arrows) virus sequences in comparison to selected representatives of hantaviruses associated with rodents, shrew and moles. The Maximum likelihood phylogenetic tree (Tamura-Nei evolutionary model) is based on partial S-segment nucleotide (418 nucleotides) sequences and calculated with MEGA5. Shrew- and mole-associated hantaviruses are indicated by light gray circles. Rodent-associated viruses are indicated by dark gray circles.

2 Aims of the study

DOBV is the most virulent hantavirus in Europe with case fatality rates up to 12%. Besides, there are several lineages of DOBV which are carried by different natural host reservoirs. When transmitted to humans they can cause mild to moderate forms of HFRS. In addition, it has been shown that two lineages could be reassorted in vitro and in nature. Therefore, DOBV is a unique hantavirus prompting to study its molecular characteristics and evaluate pathogenicity potential of different lineages to humans.

In Germany, DOBV is endemic in the north-eastern part of the country. Clinical cases of human diseases caused by DOBV are reported regularly, however, the causative agent of such illness was not identified before. Thus, we initiated the current study with the main goal to isolate and characterize the indigenous DOBV from Germany.

Aims of the study were:

1. Generate cell culture isolate of DOBV from North-Eastern Germany
2. Complete genetic characterization of virus genome
3. Complete molecular phylogenetic analyses
4. Identify cellular receptor(s) necessary for virus entry
5. Study the activation of selected innate immunity markers

It has been reported that pathogenic and non-pathogenic hantaviruses utilize distinct cellular receptors in order to maintain virus entry. Also the differential cellular interferon response to hantaviruses has been considered as one of the pathogenicity characteristics. Therefore, receptor usage and induction of innate immunity markers (tasks 4 and 5) have been taken as pathogenicity determinants of the investigated viruses. We also wanted to evaluate the pathogenicity potential of the novel, recently isolated SANGV from Africa. Partial molecular characteristics of SANGV have been published before the current work. Therefore, we concentrated our efforts on performance of tasks 4 and 5 with SANGV in order to evaluate its pathogenicity potential in comparison with DOBV from Germany.

Both SANGV and the new DOBV isolate are genetically closely related and belong to *Murinae*-associated hantaviruses. In addition, we expected the new DOBV to be pathogenic; however, in the case of SANGV there was only indirect evidence that it may infect humans. Therefore, it was interesting to compare DOBV and SANGV in order to estimate whether they demonstrate similar pathogenicity potential.

3 Materials and methods

3.1 Cells and viruses

Vero E6 (african green monkey epithelial kidney cell line; Vero C1008 ATCC CRL 1586), A549 cells (human epithelial lung cell line; ACC 107, German Collection of Microorganisms and Cell Cultures, Braunschweig, Germany) and HUH7 (human hepatoma cell line; Health Science Research Resources Bank, Osaka, Japan) were cultured in Minimal essential medium (MEM) with Earle's Salt supplemented with 5% fetal calf serum (FCS; Perbio (Bonn, Germany), 25 mM HEPES, 1% glutamine, 1% sodiumpyruvate, 1% non-essential amino acids (Biochrom AG, Germany) and 0.1% gentamycinesulphate (Bio – Wittacker, Germany).

Stocks of GRW/Aa (isolated within this study), HTNV 76–118 (kindly provided by Dr. Åke Lundkvist), PHV type 3571 (kindly provided by Dr. Robert B. Tesh) and SANGV (kindly provided by Dr. Boris Klempa) were produced in Vero E6 cells cultivated in 75 cm^2 cell culture flaks. The cells were infected at the multiplicity of infection (MOI) 0.1 for 1 hour at 37°C in 5% CO_2 humidified atmosphere, then 15 ml of fresh medium was added. After seven days, cell culture supernatants were collected, centrifuged to remove cell debris, aliquoted and stored at -80°C.

Experiments with infectious GRW/Aa, HTNV, PHV and SANGV were performed under biosafety level 3 conditions in the Institute of Virology, Charité School of Medicine.

Virus stocks and cells were determined to be free of mycoplasma contamination by using the PCR-based VenorGeM mycoplasma detection kit (Minerva Biolabs, Germany).

3.2 Virus ultracentrifugation

For production of high-titer, IFN-free virus stocks 175 cm^2 cell culture flasks were infected and incubated for seven days at culture conditions. After two freeze/thaw cycles, cells were scraped from culture vessel bottom and exposed to sonication. Cell debris was removed by centrifugation. Supernatant was transferred into sealed tubes and ultracentrifuged for 3 hours at 28,000 g and 4°C. Virus pellets were resolved in fresh culture medium through repetitive vortexing and sonication.

3.3 Inactivation of hantaviruses by UV irradiation

Virus stock solution (0.5 ml) was transferred to a small plastic Petri dish and placed directly on the workspace of the UV transilluminator equipped with 8-W tubes (Vilber Lourmat, France). Inactivation was performed by UV irradiation for 3 min at 312 nm, corresponding to 1.4 J/cm^2 [105].

3.4 Virus titration

To determine the virus titers of the viral stocks, the modified chemiluminescent focus assay described by [106] was used. Briefly, confluent Vero E6 cells grown in 6-well plates were inoculated with 0.2 ml/well of tenfold dilutions of viral stock in Hanks' balanced salt solution (HBSS) supplemented with 2% HEPES (Gibco/Invitrogen, Germany), 2% FCS and antibiotics mixture PSN (Biochrom AG, Germany). After virus adsorption for one hour at 37°C in a humidified 5% CO_2 atmosphere, the cells were overlaid (2.5 ml overlay per well) with a 1:1 mixture of 2.4% Avicel (FMC Biopolymer, USA) in water and basal Eagle´s medium (2x BME) supplemented with 5% FCS, 2.5% HEPES and antibiotics. Plates were then incubated for 7–10 days (dependent on the virus strain) under the conditions described above. Afterwards, the overlay was removed by gently pouring of washing buffer (PBS supplemented with 0.15% Tween-20) onto the overlay. By flipping the plate, the overlay was discarded. The cells were carefully washed twice with washing buffer, then fixed with methanol (1-3 ml/ well) for 8 min, allowed to dry and again washed two times. 1 ml of corresponding rabbit polyclonal antiserum was added to each well, diluted in PBS containing 10% FCS, and incubated for 1 h at 37 °C. Cell were washed five times and 1 ml of goat anti-rabbit IgG conjugated with horseradish peroxidase diluted 1:1000 in PBS supplemented with 10 % FCS was added per well and incubated for 1 hour (h) at 37 °C. Following five additional washing steps, 0.5 ml/well of the chemiluminescence substrate, Supersignal West Dura (Pierce, USA), was added. The plates were evaluated in DIANA Chemiluminescence System (Raytest, Germany). For evaluation of the titers, the focus forming units (FFU) of each well were counted and the titers were calculated per ml.

3.5 Cell culture isolation procedure

DOBV RT-PCR-positive lung samples from three naturally infected Apodemus mice trapped in a region near Greifswald/north-eastern part of Germany were used for virus isolation attempts. The samples (ca 8-10 mm^3) were processed as 10% tissue suspensions in 1 ml of Dulbecco's medium (DMEM) supplemented with 0.2% bovine serum albumin (BSA). The tissues were triturated in a closed mechanical blender FastPrep Instrument (BIO 101 Systems, Carlsbad, CA, USA). Triturated tissues were briefly centrifuged at low speed to remove larger tissue fragments and inoculated (1 ml/ flask) onto cultures of confluent Vero E6 cells in 25 cm^2 flasks. Cells inoculated with 1 ml medium only served as a negative control. Virus was then allowed to adsorb at 37°C in a humidified 5% CO_2 atmosphere. The cell culture medium (MEM plus 10% FCS, 1% L-glutamate, 100 IU penicillin and 100 µg/ ml streptomycin) was changed for the first time after 90 min and then weekly. In 2 week intervals, cells, detached

by trypsin treatment, were passaged into new culture flask with the addition of the same amount of fresh uninfected cells according to a described protocol [95]. While suspended, several slides were prepared and examined for characteristic hantavirus antigen expression following immunofluorescence assay (IFA) techniques. First positive IFA slide was observed after six weeks of cultivation. At the same time isolation attempts were stopped, the medium from positive flask was collected and used for further propagation of virus.

3.6 Immunofluorescence assay

Cells were prepared on Teflon-coated slides with 12 circular areas ("spots"). After detaching with trypsin treatment, the cells were suspended in cell culture medium and washed twice. Washed cells from every flask were resuspended in 5 ml of cell culture medium and 20 µl of the suspension was deposited on each spot of the slides cleaned with 70% ethanol. The slides were put in a moist chamber and incubated at 37°C and 5% CO_2 overnight. The slides were washed two times in PBS and once in bi-distillated water and anhydrous acetone and then fixed in anhydrous acetone at 4°C for 10 minutes, air-dried and used or stored at -20°C.

Slides were first washed before usage in PBS and air-dried. 20 µl of anti-DOBV/HTNV rabbit antisera [107] diluted 1:20, 1:40, 1:80, 1:160 and 1:320 in PBS were deposited on different spots and incubated at room temperature for 30 min in a moist chamber. The slides were washed, with 3 changes of PBS each for 5 min, and air-dried. Fluorescein isothiocyanate (FITC)-conjugated anti-rabbit immunoglobulin (Dako, Denmark), diluted 1:40 in PBS, was added, 20 µl to each spot, and the slides were returned to the moist chamber at room temperature for 30 min. To increase the contrast in staining Evan's blue (Parc Technologique Delta Sud, France) at dilution 1:1500 was added to the conjugate. The slides were again washed, with three changes of PBS each for 5 min, and air-dried. The slides were mounted with the mounting medium (Progen, Germany) under cover slips and examined for characteristic cytoplasmic pattern in a fluorescence microscope (Olympus BX60, Germany).

3.7 RNA extraction

3.7.1 RNA extraction from cell culture supernatant

For isolation of viral RNA from cell culture supernatant, the QIAmp Viral RNA Mini Kit (Qiagen, Germany) was used. The RNA was extracted according to the standard QIAmp viral RNA mini spin protocol. Briefly, 140 µl of cell culture supernatant was added to 560 µl AVL buffer containing carrier RNA and incubated at room temperature for 10 minutes. Ethanol was added to the lysate and the lysate was applied to the column provided and centrifuged. RNA was then washed with washing buffers AW1 and AW2. An additional centrifugation

step was performed to remove possible residues of the buffers. 60 µl AVE buffer were then added into the column, incubated for 1 min and the RNA was eluted by centrifugation. The RNA was stored at -20°C until further use.

3.7.2 RNA extraction from cell culture

Total RNA from cells was isolated with RNeasy Mini Kit (Qiagen, Germany). The RNA extraction was performed according to the protocol described by manufacturer. Briefly, up to 1 x 10^7 cells were lysed in RLT buffer. 70% ethanol in DEPC-water was added to the lysate and the mixture was applied to the RNeasy Mini spin column and centrifuged. Three washing steps (1 time buffer RW1, two times buffer RPE) were performed. The RNA was then eluted in 50 µl RNase-free water. 10µl of extracted RNA was directly reverse transcribed. The rest from RNA sample was stored at -20°C.

3.8 Reverse transcription

3.8.1 M-MLV Reverse transcription with the random hexamer primers

The extracted viral RNA was reversely transcribed to cDNA using N6 random hexamer primers (Invitrogen, Germany). For each reaction, 10 µl total RNA plus 10 µl PCR Mix were used. PCR Mix includes: First-Strand Buffer (100 mM Tris-HCl (pH 8.3), 150 mM KCl, 6 mM $MgCl_2$), 1 mM DTT, 0.75 mM dNTP, 25 ng of N6 primer, 100 Units of Moloney Murine Leukemia Virus Reverse Transcriptase (M-MLV RT) and 20 Units of RNaseOUT™. The reverse transcription PCR conditions were 10 min of 25°C, 30 min of 42°C, 6 min of 96°C, followed by final cooling to 4°C in the Master cycler personal (Eppendorf, Germany).

3.8.2 SuperScript III First-Strand Synthesis System for reverse transcription

The SuperScript III First-Strand Synthesis System (Invitrogen, Germany) was used in cases when amplification of long PCR products was needed (sequencing of M- and L-genome segments). Mix 1 (10µl) contains: 8 µl of RNA, 50 ng of N6 random hexamers, 1 mM dNTP mix; Mix 2 (10µl) contains: RT buffer (40 mM Tris-HCl (pH 8.4), 100 mM KCl), 10 mM $MgCl_2$, 20 mM DTT, 200 Units of Superscript III RT™ and 40 Units of RNaseOUT™.
Both mixes were prepared in separate tubes. First, Mix 1 was prepared and incubated at 65°C for 5 min and then incubated on ice for at least one minute. Then, Mix 2 was added and the tubes were placed in the Master cycler personal (Eppendorf, Germany) and the PCR reaction was started. The reverse transcription PCR conditions were 60 min of 48°C, 5 min of 85°C, at least 1 min of 4°C, addition of 1 µl of RNase H to each reaction tube, 20 min of 37°C, following final cooling to 4°C.

3.9 PCR

3.9.1 Hantavirus screening S- and L-PCR

Total RNA from cell culture supernatant was reversely transcribed with random hexamer primer (M-MLV reverse transcription kit, chapter 3.8.1). 5µl of cDNA was then used for the 1st PCR reactions.

A standard nested set of generic primers specific for the hantavirus S- and L-RNA genome segments was used for the initial screening. Two different nested PCR sets (one is to detect S-segment, another is to detect L-segment) were used for the detection of DOBV. For primer sequences, see the Table 3. The thermal cycling conditions of both 1st PCRs (40 cycles) and nested PCRs (25 cycles) were: single step of 95°C for 15 min, 59°C for 30 sec, 52/ 55°C for 60 sec (S- / L-PCR) and 72°C for 60 sec, followed by one cycle of final extension for 6 min at 72°C. PCR mixture (50 µl) contains: balanced $(NH_4)_2S0_4$, 1.5 mM $MgCl_2$, 0.1% Tween 20®, 0.2mM of each dNTP, 1µM of each primer and 5 Units of TEMPase Hot Start DNA Polymerase (Biomol, Germany).

Table 3: List of PCR primers used for hantavirus screening

PCR	Primer name	Primer sequence
S-segment 1st PCR	D113 (113-137) D1162c (1142-1162)	5'-GATGCAGAIAAICAITATGARAA-3' 5'-AGTTGIAT(I+C)CCCATIGA(I+C)TGT-3'
nested PCR	D357 (357-376) D955c (935-955)	5'-GAIATTGATGAACCIACAGG-3' 5'-ACCCAIATTGATGA(I+C)GGTGA-3'
L-segment 1st PCR	HAN-L-F1 (3119-3139) HAN-L-R1 (3550-3570)	5'-ATGTAYGTBAGTGCWGATGC-3' 5'-AACCADTCWGTYCCRTCATC-3'
nested PCR	HAN-L-F2 (3170-3192) HAN-L-R2 (3538-3559)	5'-TGCWGATGCHACIAARTGGTC-3' 5'-GCRTCRTCWGARTGRTGDGCAA-3'

The positions of primer binding sites for hantavirus specific S-PCR / L-PCR refer to the DOBV/Esl862/Aa/97 / DOBV/SK/Aa strain sequences (AJ269550 / GU904039.1). R=A+G, Y=C+T, M=A+C; S=G+C; K=G+T; W=A+T; I=inozine.

3.9.2 PCR for sequencing of DOBV complete S-, M- and L- segments

For sequencing of the complete genome, viral RNA was extracted from cell culture supernatant (chapter 3.7.1) and reverse transcribed with random hexamer primer (SuperScript III First-Strand Synthesis System for the Reverse transcription, chapter 3.8.2)

The complete S-segment sequence was obtained by sequencing of two overlapping PCR products (primer pairs: RT-DOB/D955c, MurS 598F/ RT-DOB). PCR primers are listed in

Table 4. The same approach was used to obtain the complete M-segment (primer pairs: DOB-M11/ M970R, M905F/ M1990R, M1674/ M3618).

PCR (40 cycles) conditions were similar to those described in the chapter 3.9.1, only annealing temperature (52-55°C) and elongation time (1-2 min) were always modified according to melting temperature of primers and length of the amplified fragment.

In the case of L-segment, the nested PCR amplifying overlapping L-segment fragments was carried out with PCR Extender System (5 Prime, Germany), following the application protocol of the manufacturers. The buffer of PCR was High Fidelity Buffer with 2.5 mM Mg^{2+}, provided by manufacture. 1st PCR primer pairs: MURL-1F / HAN-L-R1, HAN-L-F1 / HTND-U1; nested primer pairs: MURL 38F / HAN-L-R2, HAN-L-F2 / HTND-U1. Concentration of each primer in PCR mixture was 0.4 µM. The cycling conditions of both 1st PCRs (40 cycles) and nested PCRs (25 cycles) were: single step of 94°C for 2 min, 94°C for 20 sec, 48/ 50°C for 20 sec (1st / nested PCR) and 68°C for 2.5 min, followed by one cycle of final extension for 7 min at 68°C.

Table 4: List of PCR primers used for DOBV sequencing

PCR	Primer name	Primer sequence
S-segment PCR.1	RT-DOB (1-22) D955c (935-955)	5'-ttctgcagTAGTAGTAKRCTCCCTAAARAG-3' 5'-ACCCAIATTGATGA(I+C)GGTGA-3'
S-segment PCR.2	MurS 598F (598-618) RT-DOB (1-22)	5'-TGAARGCWGAIGARATIACAC-3'
M-segment PCR.1	DOB-M11 (11-29) M970R (950-970)	5'-CTCCGCAAGAAATAGCAGT-3' 5'-GTTTGCTGCATTTGCAGTGTG-3'
M-segment PCR.2	M905F (905-923) M1990R (1970-1990)	5'-GTTGCAACTTATTCAATTG-3' 5'-TCIGMTGCISTIGCIGCCCA-3'
M-segment PCR.3	M1674 (1674-1698) M3618 (3618-3638)	5'-TGTGAIRTITGIAAITAIGAGTGTGA-3' 5'-GCAAGATATAGAAATACCCAC-3'
L-segment 1st PCR.1	MURL-F1 (1-18) HAN-L-R1 (3550-3570)	5'-TAGTAGTAGACTCCSKAA-3' 5'-AACCADTCWGTYCCRTCATC-3'
nested PCR.1	MURL 38F (38-57) HAN-L-R2 (3538-3559)	5'-ATGGADAAATAYAGAGAAAT-3' 5'-GCRTCRTCWGARTGRTGDGCAA-3'
L-segment 1st PCR.2	HAN-L-F1 (3119-3139) HTND-U1 (6512-6533)	5'-ATGTAYGTBAGTGCWGATGC-3' 5'-TAGTAGTAGTATGCTCCGGAAA-3'
seminested PCR.2	HAN-L-F2 (3170-3192) HTND-U1 (6512-6533)	5'-TGCWGATGCHACIAARTGGTC-3'

Small letters in primer sequences indicate 5'-tails of heterologous sequence integrated for cloning or sequencing purposes. R=A+G, Y=C+T, M=A+C; S=G+C; K=G+T; W=A+T; I=inozine. The positions of primer binding sites for hantavirus specific PCR refer to the DOBV/Esl862/Aa/97 strain sequences.

3.10 Cloning and sequencing

The amplified PCR products were cloned into the pSC-A PCR cloning vector from StrataClone PCR Cloning Kit (Stratagene, Canada) according to the instructions of the manufacturer. At least three recombinant plasmids were sequenced in both directions with either respective primer pairs listed in Table 4 or M13uni / M13rev primers (Big dye Terminator V1.1 Kit, Applied Biosystems, Germany). Plasmids were then purified by the QIAGEN plasmid purification Mini Kit (Qiagen, Germany) according to the protocol of the manufacturer. Dideoxy sequencing was performed on a 3130 Genetic Analyzer sequencer (Applied Biosystems, Germany) using the Big dye Terminator V1.1 Kit (Applied Biosystems, Germany) as described by the manufacturer.

3.10.1 Long PCR Product Sequencing (LoPPS)

To sequence the full-length L-segment of newly isolated virus, a shotgun-based approach to sequence long PCR products was used [108]. Briefly, the method relies on ultrasonic shearing of PCR products, resulting in fragments 700–1.000 nt long. Termini are subsequently repaired to obtain blunt ends and 3'-A-overhangs are added before TA cloning. A predetermined number of clones are sequenced using an insert-independent primer to obtain an overlapping contig covering the full length of the PCR product.

3.10.2 Sequencing of 5'- and 3'- ends of the S-, M- and L-segments

The total RNA was extracted from Vero E6 cells infected with DOBV (MOI 0.1; 7 days post infection) according to the method described in the chapter 3.7.2.

To get 5'- and 3'- ends of particular segment ligated, the T4 RNA ligase kit (Fermentas, Germany) was used accordingly to the instructions of the manufacturer. 50 µl of reaction mixture contained: 20 µl of RNA, 50 mM Tris-HCl (pH 7.5 at 25°C), 10 mM $MgCl_2$, 10 mM DTT, 1 mM ATP, 5 µg of BSA, 40 Units of RNaseOUT™ and 50 Units of T4 RNA ligase. The mixture was incubated for 90 min at 37°C.

Ligated RNA was reversely transcribed as described in chapter 3.8.1.

To sequence ends of different segments, PCR products were obtained with a nested set of primers specific for the hantavirus S, M, and L genome segments. Thermocycler conditions were similar to described in the chapter 3.9.1, only annealing temperature for the 1st PCR / nested PCR was always 55°C. PCR products were sequenced with protocol described in the chapter 3.10. For primer sequences, see the Table 5.

Table 5: List of PCR primers used for DOBV segment ends sequencing

PCR	Primer name	Primer sequence
S-segment 1st PCR	SKS-1380F (1380-1400) SKS-132R (113-132)	5'-TGTAATCCCACATATGCTGC-3' 5'-CATACTGCTTTTCTGCATCC-3'
nested PCR	SKS-1490F (1490-1511) SKS-108R (89-108)	5'-TAATCTCAGGGTGGGTTAGGA-3' 5'-CCTTCTGCCTGGCTATCACC-3'
M-segment 1st PCR	SKM3311F (3309-3331) DOBM 970R (950-970)	5'-GGTTTATAAAATCTGGAGAGTGG-3' 5'-GTTTGCTGCATTTGCAGTGTG-3'
seminested PCR	SKM3311F (3309-3331) SKM-146R (146-166)	5'-ACCTGTTACACTGCTCTCTCC-3'
L-segment 1st PCR	SKL orf 6032F (6033-6052) DOB L 669R (650-669)	5'-GGGTGACTTGCTTATCATGT-3' 5'-AACATKGCYTCYARAGCAGC-3'
nested PCR	GRW-L-6339F (6339-6367) GRW-L-591R (563-591)	5'-AGTTTAGCACATTTGATCAGGAGGCACAG-3' 5'-CTCATGTATTGAACAACCCCGTCATTTCT-3'

The positions of primer binding sites for hantavirus specific PCR refer to the DOBV/Esl862/Aa/97 strain sequences.

3.11 Sequence comparison and phylogenetic analysis

The obtained overlapping nucleic acid sequences were combined for analysis and edited with the aid of the SEQMAN program from the Lasergene software package (DNASTAR, Madison, Wis.). The sequence data were further analyzed by using the BioEdit software package [109]. Sequences were aligned by using CLUSTAL W, implemented in BioEdit software, with default parameters. The sequences were first aligned on amino acid level and then reverse translated to nucleotide sequences by using BioEdit software. The reliability of the alignment was checked by using DotPlot analysis provided by BioEdit software package. The alignment was tested for phylogenetic information by Likelihood Mapping analysis [110]. To reconstruct maximum-likelihood (ML) phylogenetic trees, we applied quartet puzzling by using the TREE-PUZZLE package [110,111]. As an evolutionary model for the reconstructions, the Tamura-Nei model was used; missing parameters were reconstructed from the datasets. Values above the branches represent PUZZLE support values. Values below the branches are bootstrap values of the corresponding ML phylogenetic tree (Tamura-Nei evolutionary model) calculated with the MEGA5 software [112] from 1000 bootstrap pseudoreplicates. Resulting evolutionary trees were then visualized by using MEGA5 software [112].

3.12 Receptor blocking assay

Antibodies against α5β1 integrin, mouse monoclonal antibody MAB1969, (Millipore, Germany), αvβ3 integrin, mouse monoclonal antibody MAB1976 (Millipore, Germany) and DAF/CD55, rabbit polyclonal antibody H319 (Santa Cruz, Germany), were added to the confluent Vero E6 cells (seeded in 12 well plates). Cells were treated with 40 µg/ml of antibodies for 1 h at 4°C. Thereafter the virus (MOI 0.05) was added to the monolayer. After incubation for 1 h at 37°C, the cells were washed with medium and incubated for 24 h under growth conditions. Samples were taken for qPCR and Western Blot analysis. The percentage of antibody-mediated inhibition of infection (viral RNA production measured by qPCR) was calculated in comparison to untreated, infected cells. The density of N-protein and β-actin (reference protein) bands on Western blot were quantified by ImageJ 1.41o program (Wayne Rasband National Institutes of Health, USA). The expression of N-protein was normalised to the expression of β-actin. The percentages of antibody-mediated inhibition of viral infection (N-protein expression) were calculated in comparison to untreated but infected cells. Data are summarised in the graphical way.

3.13 Quantitative real time PCR (qPCR)

A549 cells or HUH7 cells were seeded in 12-well plates at a density to achieve 90–95% confluence after overnight incubation at culture conditions. For poly I:C-treatment, cells were transfected for 6 hours with 1.6 µg/well of poly I:C, high molecular weight #tlrl-pic (InvivoGen, USA) and Lipofectamine 2000 (Invitrogen, Germany). Cells were infected with MOI 1, at indicated time points RNA was isolated using the RNAeasy kit (Qiagen, Germany). Extracted RNA was subjected to the DNAse digestion (RNAeasy MinElute Cleanup Handbook 10/2010, Appendix C), following the protocol provided by manufacturer (Qiagen, Germany). Purified RNA was reversely transcribed by M-MLV Reverse transcription kit with the random hexamer primers (Invitrogen, Germany). MxA-, IFN-ß- and IFN-λ1-relative gene expression (quantified as fold induction of the gene in infected or stimulated cells in comparison to uninfected or untreated cells (negative control)) was quantified by QuantiTest Sybr Green PCR kit (Qiagen, Germany). Each PCR reaction contained 4 µl of corresponding cDNA, 0.4 µM final concentration of each corresponding primer in a 20 µl of total reaction volume. PCR conditions were taken from manufacturer protocol; annealing temperature for MxA and IFN-ß primers was 55°C, and 59°C for IFN-λ1 primer pairs. Using the Pfaffl method [113,114], data are presented as the fold change in gene expression normalized to an endogenous housekeeping gene (PBGD) and relative to the untreated control. Annealing

temperature and primers for PBGD qPCR were adapted from previously published protocol [115].

qPCRs for GRW/Aa, HTNV, SANGV and PHV viral S-segments RNA were performed as previously described [116]. The viral RNA was quantified by using S-segment templates of known copy numbers. Virus genome copy numbers were normalized to ng of total cellular RNA. The list of primers and probes used in qPCR assays is attached in Table 6.

Experiments were repeated three times, each repetition included infections/transfections performed in duplicates. Results are presented as the mean ± standard deviation of the mean.

Table 6: Primers and probes used in real-time SYBR Green and TaqMan qPCR

Real Time PCR	Primer/ Probe name	Primer / Probe sequence
MxA	MxAq F MxAq R	5'-GAGGAGATCTTTCAGCACCTGAT-3' 5'-CTGGATGATCAAAGGGATGTGGC-3'
IFN-ß	IFNb se IFNb as	5'-GCCGCATTGACCATCTATGAGA-3' 5'-GAGATCTTCAGTTTCGGAGGTAAC-3'
IFN-λ1	IFN L1 F IFN L1 R	5’-GTCACCACAGGAGCTAGCGA-3’ 5’-GTGAAGGGGCTGGTCTAGG-3’
PBGD	PBGD F PBGD R	5'-GGCTGCAACGGCGGAA-3' 5'-CCTGTGGTGGACATAGCAATGATT-3'
DOBV-S-segment	DOBV F DOBV R DOBV R1 Probe (DOBV TMGB)	5'-GACTCACCRTCATCAATYTGGGT-3' 5'-TGGAGGACAGMAAARAATGCACC-3' 5'-GATGCCATGATIGTRTTCCTCAT -3' 5'-F-TCTGCCATGCCTGC--MGB-3'
SANG-S-segment	lcSA14-F1 lcSA14-R1 Probe (SA14-TAQ)	5'-AGGCTGTCAGACAACAAGCA-3' 5'-GCTCCTGCAAATACCCAAAT-3' 5’-F-TGGACCACATTGACTCACCATCATCA-TMR-3’
HTNV-S-segment	Ht&Se F Ht&Se R Probe (Hat&Se MGB) Probe (Hat&Se MGB1)	5'-CATGGCWTCHAAGACWGTGGG-3' 5'-TTKCCCCATGCCACCAT-3' 5'-F-TCAATGGGGATACAACT--MGB-3' 5'-F-TCAATGGGAATACAACT--MGB-3'
PHV-S-segment	lcPHVF lcPHVR Probe (PHV-TAQ)	5'-AGGAAGAGATCACTCGCCAT-3' 5'-TCCAATGTTGACACTGCTGA-3' 5’-F-CATTGCCCGGCAGAAGCTCA--TMR-3’

F = FAM label, **TMGB** = hydrolysis probe coupled to an MGB moiety; **MGB** = Minor Groove Binder, **TMR** = TAMRA, **R** = antisense orientation, **F** = sense orientation, location of the oligonucleotide in reference to the respective GenBank entry.

3.14 ELISA of IFN-λ1

ELISA was performed using the human IFN-λ1 DuoSet ELISA Development System (R&D Systems, DY1598) as in the recommended protocol, with the exception of coating the plates with a polyclonal anti-human IFN-λ1 capture antibody (R&D Systems, AF1598). This antibody was used for its greater cross-reactivity to African green monkey-derived IFN-λ. 96-well plates were precoated for 16 hours at 4°C with 100 µl of a polyclonal anti-human IFN-λ1 capture antibody (2 µg/ml). After capture antibody was bound to plate, 300 µl of 3% BSA (diluted in PBS) were added in order to block unspecific bindings, plate was incubated at room temperature for 1 hour. Thereafter, wells were washed four times with a washing buffer (1% BSA in PBS). Samples, containing 100 µl of Vero E6-derived viral stocks or Vero E6-conditioned medium as a control that had been subjected to UV irradiation, were added and incubated for 2 hours at room temperature. Wells were washed again and 100 µl of detection antibody (400 ng/ml) were added and incubated for 2 hours at room temperature. After that wells were washed again with a washing buffer and 50 µl of Streptavidin-HRP (0.5 µg/ml) were added and incubated at room temperature for 30 minutes. Wells were washed 4 times with washing buffer and 50 µl of TMB Substrate Solution (Seramun Diagnostica, Germany) were added and incubated at room temperature for 10 minutes, followed by addition of 50 µl of Stop Solution (1N H_2SO_4). Optical density (O.D.) of each well in the plate was measured on the reader (Sunrise Tecan, Switzerland) at 450 nm. The concentrations of IFN-λ1 were interpreted from a curve generated using 2-fold dilutions of a recombinant IFN-λ1 standard starting at 4000 pg/ml. All data were reported as the average of samples and standards run in duplicate wells.

3.15 Protein chemistry

3.15.1 Western blot

Cell extracts were prepared by lysing the cells with sample buffer (250 mM Tris, 2% SDS, 10% Glycerin, 5% ß-mercaptoethanol, 25 U/ml of Benzonase and 0.01% bromphenolblue) at 37°C for 5 min. To remove cell debris, the lysate was centrifuged and afterwards boiled at 95°C for denaturing of the proteins. For separation of the proteins, samples were loaded on a 10% polyacrylamide gel. The gel was run at 25 mA/gel until the blue front was at the bottom of the gel.

Table 7: Composition of SDS gels for Western blot analysis

Chemicals	10% Resolving gel	5% Stacking gel
30% Acrylamide/Bis (29:1)	8.3 ml	1.3 ml
1.5M Tris HCl (pH8.8)	6.5 ml	---
0.5M Tris HCL (pH 6.8)	---	2.5 ml
H_2O	9.9 ml	6.1 ml
10% SDS	200 µl	200 µl
10% APS	250 µl	50 µl
TEMED	25 µl	10 µl

Following electrophoretic separation, proteins were transferred onto methylcellulose membrane by semi-dry blotting method at 75 mA/gel. The resolving gel was cut from the stacking gel. Three pieces of Whatman paper were soaked with blotting buffer and placed onto the semi-dry electroblotting device. The gel was placed onto the Whatman paper. The nitrocellulose membrane was equilibrated in the semidry blotting buffer and placed onto the gel. Finally three additional Whatman papers were put onto the membrane. The transfer was performed for one hour at 75 mA/gel. After the transfer, the gel was stained with Coomassie Brilliant Blue staining to visualize the efficiency of protein transfer. Then the blots were blocked for 1 hour at room temperature in TBST (100 mM Tris-HCl (pH 8.0), 1.5 M NaCl, 0.5 % Tween 20) containing either 5% milk powder or 5% BSA (in the case of phosphorylated protein of interest). Specific primary antibodies, diluted in TBST containing 2% milk powder (2.5% BSA), were added to the blots and incubated for 1 hour to 12 hours at 4°C. The membranes were then washed five times with TBST, followed by incubation with appropriate secondary antibodies conjugated with horseradish peroxidase for 1 hour at room temperature. After five final washing steps, detection of the stained proteins was performed by adding chemiluminescent substrate (SuperSignal West Dura Extended Duration Substrate) to the membranes. The proteins were visualised by exposure on a CCD camera (Bioblock Scientific, France).

3.15.2 Detection of antiviral MxA protein, interferon-inducible PKR, elongation factor eIF2*α*, viral nucleocapsid and ß-actin (reference protein) expression

The expression of the MxA protein was examined in A549 and HUH7 cells. Cells were grown in 12-well plates and infected with MOI 1 of the respective virus. Cells infected with HTNV were taken as a positive control in MxA expression assays. Uninfected cells were taken as a negative control. Plates were incubated at 37°C in 5% CO_2 humidified atmosphere. At time points 1, 2, 3, and 4 days post infection, samples were taken for each virus. Briefly, the

medium was removed and cells were carefully washed twice with PBS. After removing the PBS, lysis buffer (see the chapter 3.15.1) was added to the cells. The plates were incubated for 15 min at 37°C. Afterwards, the lysate was transferred to 0.5 ml tube and stored at -20°C until analysis by Western blot.

Table 8: Primary antibodies for Western blot analysis

Specificity (dilution)	Origin	Reference
α – SK/Af (1:500)	rabbit	[107]
α – Sang (K105)	rabbit	Seramun Diagnostia, Germany
PKR (phospho T446) antibody [E120] (1:500)	rabbit	Abcam plc, UK
PKR (ab58301) (1:1000)	mouse	Abcam plc, UK
Phospho-eIF2α (Ser51) (119A11) (1:500)	rabbit	Cell signalling, USA
eIF2α (L57A5) (1:1000)	mouse	Cell signalling, USA
M 143 α – MxA (1:500)	mouse	[117]
ab6276 α -Actin (beta) (1:150000)	mouse	Abcam plc, UK

Table 9: Secondary antibodies for Western blot analysis

Antibody (Dilution)	Reference
horseradish-peroxidase (HRP)-labelled Goat anti-Rabbit IgG 1:1000	Dako, Denmark
horseradish-peroxidase (HRP)-labelled Goat anti-Mouse IgG 1:1000	Dako, Denmark

3.15.3 PKR inhibition assay

A549 cells were seeded in 12 well plates one day before infection, to achieve 80% confluence. Cells were infected with corresponding virus with MOI 1 for two and four days. Afterwards, cells were transfected with poly I:C in order to stimulate phosphorylation of PKR. For poly I:C-treatment, infected cells (after two and four days post infection) were transfected (accordingly to manufacturer instructions) for six hours with 0.5 µg/well of poly I:C, high molecular weight #tlrl-pic (InvivoGen, USA) and Lipofectamine 2000 (Invitrogen, Germany). Then cells were lysed in protein lysis buffer (chapter 3.15.2) and passed on to the Western blot analyses (chapters 3.15.1, 3.15.2). The inhibition effect was assessed by comparison of virus infected, poly I:C-stimulated cells with uninfected, poly I:C-stimulated cells.

4 Results

4.1 Generation of DOBV cell culture isolate from Germany

4.1.1 Virus isolation

During 2002-2008 around 400 Apodemus mice were trapped in three federal states of Germany (Lower Saxony, Mecklenburg-Western-Pomerania and Brandenburg). Tissues were obtained from both *A. agrarius* and *A. flavicollis* rodent species. DOBV-IgG ELISA revealed 20 positive samples [35]. Three animal tissues (two of *A. agrarius* and one of *A. flavicollis* origin) positive for DOBV in serology and RT-PCR (GER/08/118/Aa, GER/08/125/Aa and GER/08/131/Af) were used in the current study. Lung tissue suspensions of infected animals were inoculated onto Vero E6 cells. After six weeks of blind passaging (three passages) infected cells were detected by immunofluorescence assay in case of the GER/08/131/Af sample (Figure 10) and the presence of viral RNA in the cell culture supernatant was verified by RT-PCR (data not shown). The novel isolate was called Greifswald virus (GRW) according to the geographical region where the positive animal had been trapped.

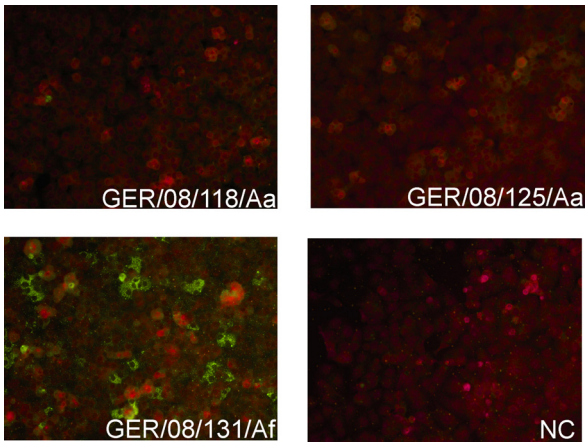

Figure 10: Evaluation of virus isolation success by immunofluorescence assay. Immunofluorescent staining of Vero E6 cells inoculated with lung tissue suspensions of RT-PCR positive mice (GER/08/118Aa, GER/08/125Aa, GER/08/131Af) and a negative control (NC) using DOBV/ HTNV human convalescent-phase serum. Evans Blue Reagent was used as a counter stain.

The fact that the cell culture isolation succeeded only in the case of a tissue from a spill-over infected rodent (see below) raised the question of determinants of successful isolation procedure. Therefore we retrospectively quantified the virus load in the used tissue samples by quantitative real-time PCR (qPCR). Indeed, the highest virus load was observed in lungs of GER/08/131/Af mouse (290 ± 94 copies per ng of total RNA) while GER/08/118/Aa and GER/08/125/Aa tissue samples were determined to contain 99 ± 62 and 0.7 ± 0.6 copies per ng of total RNA, respectively.

4.2 Complete genetic characterization of the new virus isolate

4.2.1 Sequence analysis of GRW virus genome segments

Complete nucleotide sequences of all three virus genome segments were determined. S-segment was found to be 1,675 nucleotides (nt) long and its single open reading frame (ORF; nt position 36-1,325) encodes the viral nucleocapsid protein of 429 amino acids (aa). M-segment is 3,644 nt long and encodes the glycoprotein precursor of 1,135 aa (ORF position 41-3,448). L-segment is 6,532 nt long and encodes the viral RNA-dependent RNA polymerase of 2,151 aa (ORF position 38-6,493).

Based on the current hantavirus classification, defined by the International Committee on Taxonomy of Viruses (ICTV), a distinct hantavirus species has to exhibit at least a 7% difference in amino acid identity when comparing the complete S-segment and M-segment sequences. Recently, new criteria of ICTV guidelines have been suggested for the demarcation of hantavirus into species (amino acid distance of >10% for S-segment or >12% for M-segment) [118]. According to these guidelines, GRW virus does not form a separate hantavirus species and clearly belongs to the DOBV species. The sequence similarities between GRW and other DOBV isolates were in range from 79.8 to 89.3% on nucleotide and from 90.2 to 98.8% on amino acid level (Table 10). SK/Aa showed the highest sequence identity values with more than 96% aa sequence identity for all three segments. Interestingly, for the S-segment sequences the lowest similarity values were observed for SAAV/160V while for M- and L- segment sequences for Sochi/hu.

Table 10: Complete ORF nucleotide and amino acid sequence identities of GRW with other DOBV, SANGV and HTNV isolates*

virus isolate		% identity of GRW with virus isolates					
		S-segment		M-segment		L-segment	
		nt	aa	nt	aa	nt	aa
DOBV isolates	SK/Aa	89.3	98.8	86.6	96.3	86.7	97.3
	SAA/160V	87.4	97.4	87.0	95.9	88.0	97.2
	Slo/Af	88.2	97.9	83.2	94.3	85.9	97.6
	Sochi/hu	87.7	98.3	79.8	90.2	83.4	95.8
SANGV		78.2	88.5	72.4	80.7	75.5	86.9
HTNV/76-118		74.2	83.4	70.5	76.6	74.7	85.0

* ORF, open reading frame. nt, nucleotides. aa, amino acids. NA, not available

4.2.2 Panhandle-forming terminal nucleotides (22-29 bp long) of the GRW RNA genomic segments

In order to characterize the complete genome of GRW, exact 3'- and 5'-termini of all three viral RNA segments were determined (for detailed protocol see Materials and methods section). As it has been observed for other hantaviruses [39], 3'- and 5'-termini of GRW viral RNA are forming panhandle structure with a length of 22-29 bp (Figure 11). 14 of the 22-29 bp are identical in all three segments. However, base pairing is incomplete, with two mismatches (within the 14 identical bp) at positions 9 and 10. In other hantaviruses such as HTNV, SEOV, PUUV and SNV, a noncanonical G:U pair in position 10 is present [39]. In case of GRW G:U pair appears at position 28 in S- and M-derived panhandles and at position 19 in L-derived panhandle (Figure 11).

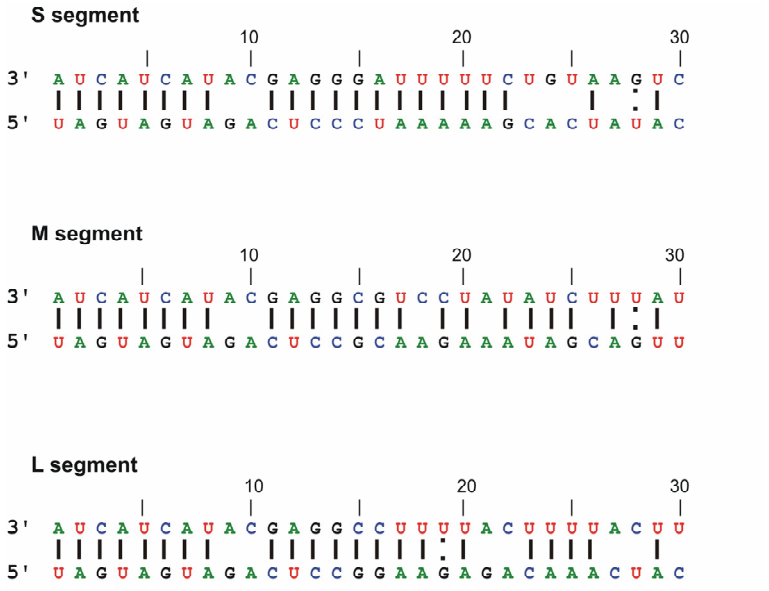

Figure 11: Panhandle-forming terminal nucleotides (22-29 bp long) of the GRW/Aa RNA genomic segments. |, complementary pairing; :, noncanonical U-G pair

4.3 Molecular phylogenetic analyses

ORF sequences of all three GRW segments were analyzed by the maximum-likelihood method with Tamura-Nei evolutionary model (Figure 12). Before the tree reconstruction used data sets were analyzed by RDP3 program with automated screening procedure [119]. No putative recombination regions for any of the used data sets could be detected by more than 3 programs implemented in RDP3.

In S- and M-segment analyses, the GRW sequences clustered with high statistical support together with DOBV sequences obtained from mice trapped in Northern Germany and therefore clearly belong to the DOBV species (Figure 12 A and B). Moreover, there was no

difference in sequences obtained from mouse tissue (GER/08/131/Af) and its cell culture-generated isolate (GRW), demonstrating the absence of mutations during cell culture isolation procedure at least for the analyzed S- and M- segment coding sequences (Figure 12). As previously stated for the rodent tissue-derived sequence GER/08/131/Af [35], the new DOBV strain was isolated from *A. flavicollis* mouse, but genetically belongs to the DOBV-Aa lineage (associated with *A. agrarius* as a natural host) (Figure 12 A, B, C). This finding shows that the virus was obtained from a spill-over infected animal. Therefore, the new DOBV isolate was designated as GRW/Aa according to its evolutionary origin in DOBV-Aa lineage and despite the fact that it was isolated from *A. flavicollis*. In addition, comparison of phylogenetic trees of all three segments revealed no indications for reassortment events of GRW/Aa with other hantavirus strains (Figure 12 A, B, C).

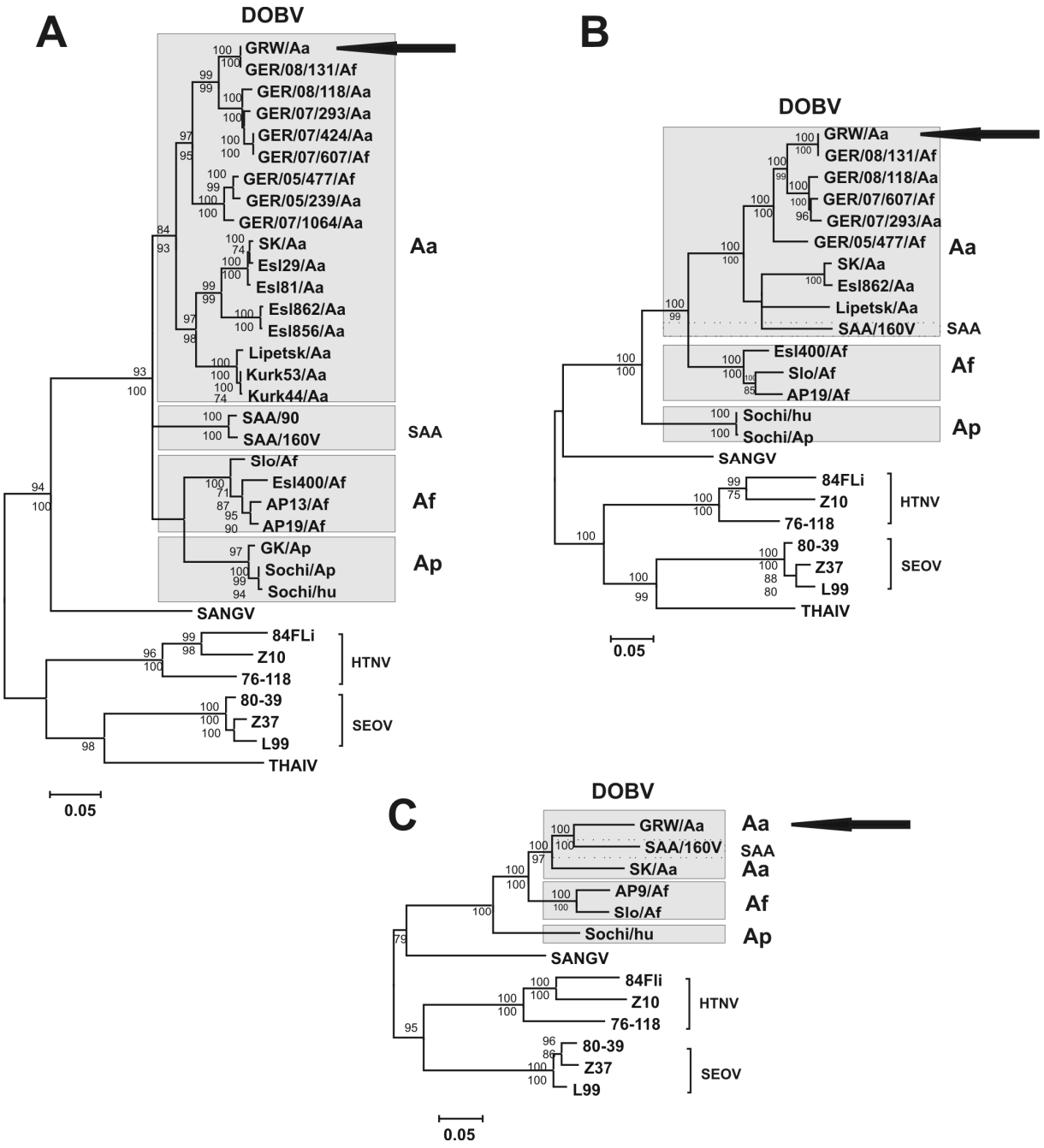

Figure 12: Maximum likelihood phylogenetic trees (TREE-PUZZLE package, Tamura-Nei evolutionary model) based on (A) complete S-, (B) complete M- and (C) complete L- segment ORFs sequences.

← - GRW/Aa positions in trees. Values above the branches represent PUZZLE support values, while values below the branches are bootstrap values of the corresponding maximum likelihood phylogenetic trees (Tamura-Nei evolutionary model) calculated with the MEGA5 software from 1,000 bootstrap pseudoreplicates. Only values > 70% (considered significant) are shown. Different DOBV clades are indicated by gray boxes. Before tree reconstruction sequence data were verified by RDP3 program [119]. No putative recombinant regions could be detected by more than 3 programs implemented in the RDP3 automated screening. For abbreviations and accession numbers, see the materials and methods.

4.4 Molecular evidence of DOBV-caused human infections in Germany

4.4.1 Clinical case of DOBV-caused HFRS from Northern Germany

In October 2010, a 35 years old woman (patient H431) from Walsleben, north of Germany, was hospitalized to the local hospital in Neuruppin. At admission, she developed symptoms compatible with a hantavirus infection, such as influenza-like symptoms, fever, headache, back and abdominal pain, acute renal failure with proteinuria.

First testing of the serum (H431) was performed in Stuttgart (Laboratory Prof. Enders) applying ELISA from Progen (Germany). Patient serum was examined to detect the presence of specific IgG and IgM antibodies to either Hantaan (HTNV) or Puumala viruses (PUUV). The test revealed the presence of HTNV-specific IgM antibodies. Knowing that antibodies against HTNV highly cross-react with DOBV, further testing was performed in order to differentiate whether patient serum react better with HTNV or DOBV antigens.

A detailed serum examination was performed by in-house ELISA in Berlin (Table 11). This ELISA uses recombinant DOBV and PUUV nucleocapsid protein antigens to detect the presence of specific IgG and IgM antibodies. The titers of IgG and IgM to DOBV antigen were determined to be 1:102,400 and 1:25,600, respectively, whereas PUUV-specific IgG antibodies could not be detected.

Table 11: Testing of serum H431 by in-house ELISA (Berlin). End-point antibody titers are shown.

DOBV-IgG	1:102,400
DOBV-IgM	1:25,600
PUUV-IgG	<1:400
PUUV-IgM	Not done

IgG antibodies were analyzed by Bunya-BLOT (Mikrogen, Germany). This BLOT uses recombinant hantavirus nucleocapsid protein antigens to detect the presence of specific IgG antibodies. Bunya-BLOT analyses revealed IgG antibodies present in patient serum which react with HTNV / PUUV and DOBV antigens (Figure 13).

Figure 13: Bunya-BLOT IgG (Mikrogen, Germany) analyses of serum from H431 patient. SC, serum control (IgG); cut-off, bands are only considered to be positive if darker than cut-off band; PUUV, Puumala virus; HTNV, Hantaan virus; DOBV, Dobrava-Belgrade virus; SEOV, Seoul virus; N, viral nucleopcapsid protein.

4.4.2 Molecular phylogenetic analyses including patient derived sequences

RNA for reverse transcription PCR (RT-PCR) was extracted from patient H431 serum. A nested PCR specific for DOBV M- and L-segments generated DNA bands of expected sizes (M, 317 nt, positions 1,673 to 1,989; L, 300 nt, positions 3,013 to 3,312). Nucleotide sequence of these fragments were determined and phylogenetically analyzed. In addition, previously published S-segment sequence derived from a patient (H169, [100]) was also included in phylogenetic analyses.

In analyses of partial S-, M-, and L- segments (Figure 14 A, B, C), Northern German HFRS patient-derived nucleotide sequences H169 (S-segment only) and H431 (M- and L-segments only) cluster closely with mouse-derived DOBV-Aa sequences and GRW/Aa. Therefore, phylogenetic analyses undoubtedly showed that sequences obtained from patient H431 are of DOBV-Aa origin. In addition, analyses demonstrated that DOBV circulating in the natural host population from this particular region is responsible for human disease. Based on obtained results, GRW/Aa can be taken as a representative for hantavirus causing HFRS in the northern part of Germany.

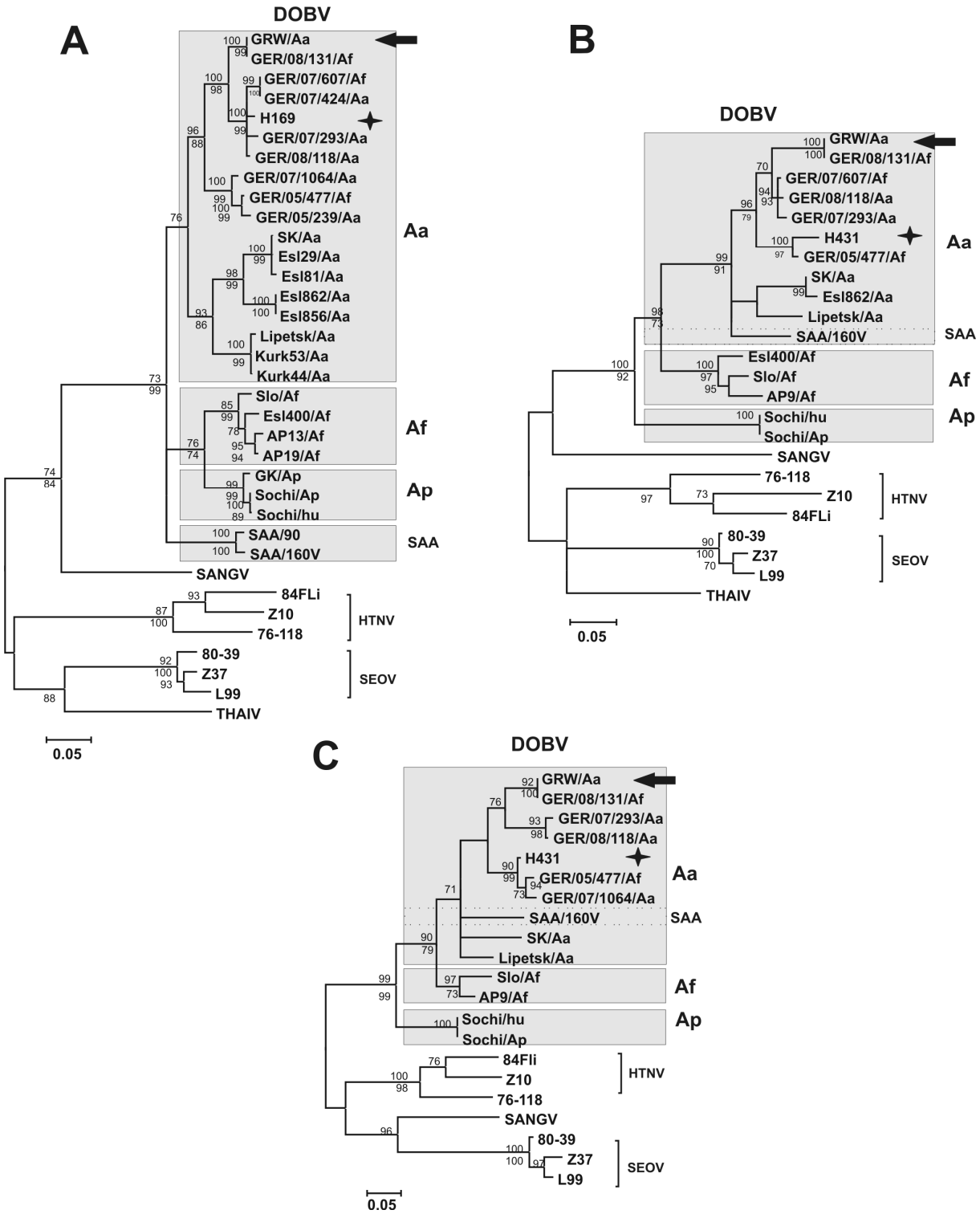

Figure 14: Maximum likelihood phylogenetic trees (TREE-PUZZLE package, Tamura-Nei evolutionary model) based on (A) partial S- (559 nt, positions 377 to 938), (B) partial M- (317 nt, positions 1,673 to 1,989), (C) partial L- (300 nt, positions 3,013 to 3,312) segment sequences.

← - GRW/Aa positions in trees. ✦ - positions of DOBV patient-derived sequences in trees. Values above the branches represent PUZZLE support values, while values below the branches are bootstrap values of the corresponding maximum likelihood phylogenetic trees (Tamura-Nei evolutionary model) calculated with the MEGA5 software from 1,000 bootstrap pseudoreplicates. Only values > 70% (considered significant) are shown. Different DOBV clades are indicated by gray boxes. Before three reconstruction sequence data were verified by RDP3 program [119]. No putative recombinant regions could be detected by more than 3 programs implemented in the RDP3 automated screening. For abbreviations and accession numbers, see the materials and methods.

4.5 Cellular receptors necessary for GRW/Aa virus and SANGV entry

As a further step towards virus characterization, the receptor usage of GRW/Aa virus was determined using blocking experiments. In parallel studies receptor usage for the novel African hantavirus, SANGV, has been assessed as well.

In Vero E6 cells, the putative hantavirus receptors (αvß3 integrin, α5ß1 integrin, DAF) were blocked by pre-incubation with specific blocking antibodies and then the cells were infected with the virus. Efficiency of the virus entry blockage was evaluated by quantification of viral RNA with qPCR (Figure 15 A) and detection of viral nucleocapsid protein by Western blot analyses (Figure 15 B) in the infected cells. In addition, HTNV and PHV were used in the assay as a control of our experimental settings since their entry was reported to be inhibited by ß3 and ß1 integrin-specific antibodies, respectively [52]. HTNV has been also found to be inhibited by anti-DAF antibodies [55]. Both approaches revealed that the presence of accessible avß3 integrin and DAF receptors on the cell surface is important for GRW/Aa entry. We observed up to 60% inhibition of GRW/Aa infection in the presence of neutralizing anti-αvß3 integrin and up to 80% of GRW/Aa inhibition in the presence of anti-DAF antibodies, whereas anti-α5ß1 antibody failed to block GRW/Aa infection.

In the case of SANGV, results of both qPCR (Figure 15 A) and Western blot (Figure 15 B) clearly indicated that SANGV infection can be efficiently blocked only by anti-α5ß1 integrin antibodies. We observed up to 80% in qPCR and up to 60% by Western blot inhibition of SANGV infection in the presence of blocking anti-α5ß1 antibodies.

As a control for our experimental settings we reproduced data confirming receptor usage of HTNV and PHV known from literature and mentioned above. Interestingly, although infection by both control viruses could be efficiently inhibited also by anti-DAF antibodies, this was not the case for SANGV which could be significantly inhibited exclusively by ß1-specific antibodies.

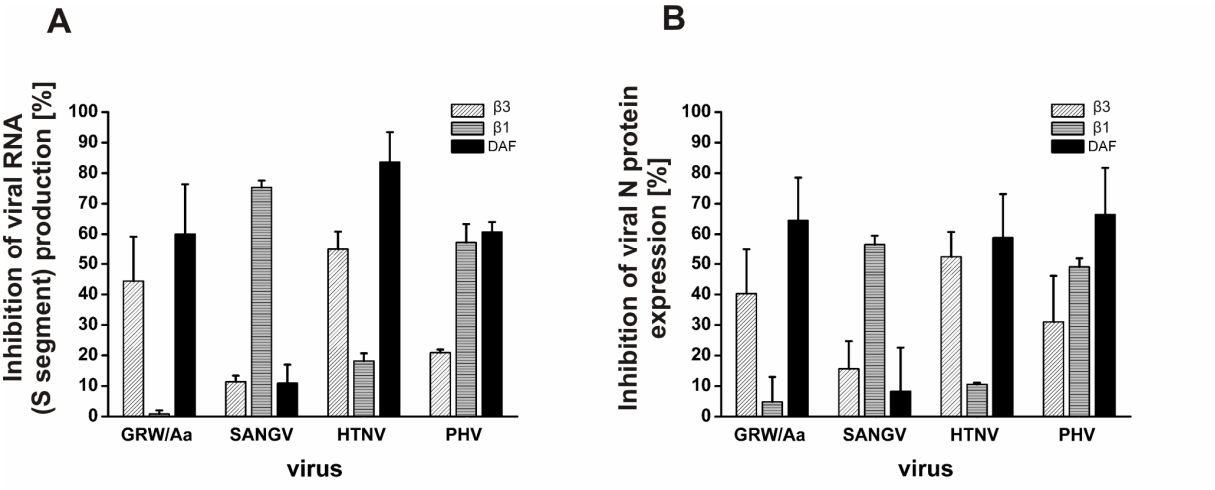

Figure 15: Integrin / DAF receptor blocking assay. Vero E6 cells were treated with 40 µg/ml of indicated blocking antibodies for one hour. Then corresponding virus at multiplicity of infection (MOI) 0.05 was added to the cells. After one hour cells were washed, new medium was added. One day later samples were collected. A) Viral S-segment RNA expression was measured by qPCR. B) Expression of viral nucleocapsid (N) protein was detected by Western blot. The density of bands on blots was quantified by ImageJ 1.41o programm (Wayne Rasband National Institutes of Health, USA). The percentages of antibody-mediated inhibition of viral infection were calculated in comparison to untreated but infected cells. Experiment was performed three times. Data are presented as the mean ± SD of the mean.

4.6 Activation of selected innate immunity markers in response to GRW/Aa and SANGV infection

4.6.1 Expression of antiviral MxA protein and mRNA in response to GRW/Aa and SANGV infection

Since A549 and HUH7 cells have been used in previous studies on innate immunity response in terms of hantavirus infection [71,120], we also elucidated how A549 and HUH7 cells respond to GRW/Aa and SANGV infection. MxA protein and mRNA expression were investigated by Western Blot and qPCR, respectively.

MxA protein expression in response to GRW/Aa infection of A549 cells was first detectable by Western blot at day 4 post infection (Figure 16 A) but MxA mRNA measured by qPCR was gradually increasing from day 1 to day 4 post infection (Figure 16 B). Interestingly, there was no detectable MxA protein expression after GRW/Aa infection in HUH7 cells (Figure 16 C). However, some basic and continuous expression of MxA mRNA (~ 10 folds induction in comparison to negative control) was observed in HUH7 cells exposed to GRW/Aa infection (Figure 16 D). Similar MxA protein expression patterns were observed for pathogenic HTNV and DOBV-SK/Aa [71,72].

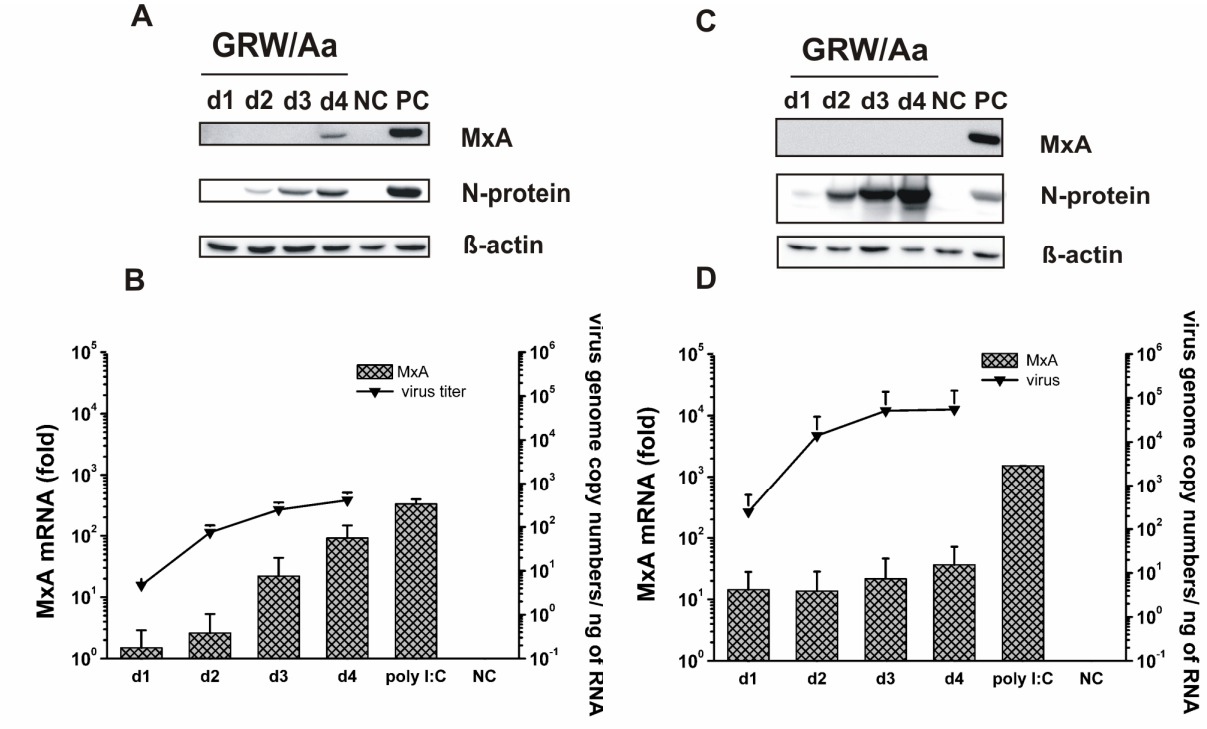

Figure 16: Monitoring of MxA protein expression and MxA, viral RNA expression in A549 cells (A, B) and in HUH7 cells (C, D) after GRW/Aa infection. A549 cells or HUH7 cells were infected at MOI 1. Samples were taken at indicated time points post infection A), C) Expression of antiviral MxA protein detected by Western blot. NC (negative control), uninfected cells. PC (positive control), cells infected with HTNV for four days. β-actin was taken as a reference protein (loading control). Representative results of two independent experiments are shown. B), D) Expression of viral RNA and induction of MxA mRNA in response to GRW/Aa infection measured by qPCR. Poly I:C, cells transfected at the time of infection with 1.6 µg of poly I:C for six hours. Experiment was performed three times. Data are presented as the mean ± SD of the mean.

MxA protein expression in response to SANGV infection of both A549 and HUH7 cells was observed already at day 1 post infection (Figure 17 A, C) and was gradually increasing from day 1 to day 4. The expression of MxA protein in HUH7 cells seems to be stronger in comparison to MxA protein expression in A549 cells infected with SANGV. Since MxA protein expression was observed already at day 1 after infection with SANGV, investigation of MxA mRNA levels by qPCR was extended to earlier time points after infection (1 hour, 6 hours and 12 hours). We observed significant induction of MxA mRNA (~ 100 folds induction in comparison to negative control) already 6 hours post infection in SANGV infected A549 and HUH7 cells (Figure 17 B, D). The obtained pattern for MxA mRNA expression in response to SANGV was almost the same in both cell lines (Figure 17). Interestingly, SANGV-mediated MxA protein expression patterns resemble patterns which were reported for non-pathogenic PHV [71].

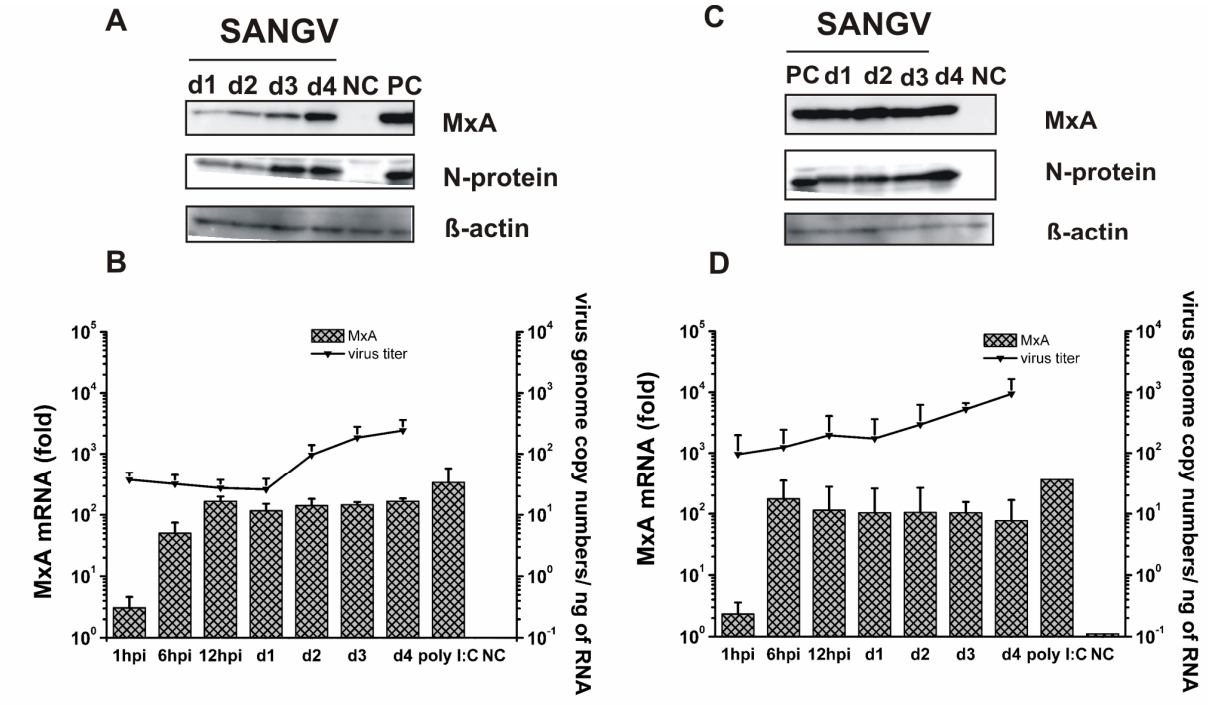

Figure 17: Monitoring of MxA protein expression and MxA, viral RNA expression in A549 cells (A, B) and in HUH7 cells (C, D) after SANGV infection. A549 cells or HUH7 cells were infected at MOI 1. Samples were taken at indicated time points post infection A), C) Expression of antiviral MxA protein detected by Western blot. NC (negative control), uninfected cells. PC (positive control), cells infected with HTNV for four days. β-actin was taken as a reference protein (loading control). Representative results of two independent experiments are shown. B), D) Expression of viral RNA and induction of MxA mRNA in response to SANGV infection measured by qPCR. Poly I:C, cells transfected at the time of infection with 1.6 µg of poly I:C for six hours. Experiment was performed three times. Data are presented as the mean ± SD of the mean.

4.6.2 IFN-ß and IFN-λ1 induction in response to GRW/Aa and SANGV infection

The observed MxA induction pattern motivated us to study further the mechanisms regulating MxA expression. Since MxA expression is tightly regulated by type I and type III interferons (IFNs) and is not induced directly by viruses or other stimuli [77], it was necessary to investigate whether GRW/Aa and SANGV induce type I IFN (IFN-ß) or/ and type III IFN (IFN-λ1) in cell lines. Given that A549 cells are established from lung epithelium which is affected during hantavirus infection, we chose A549 as a target cell line to set up methods and to study IFNs induction by hantaviruses.

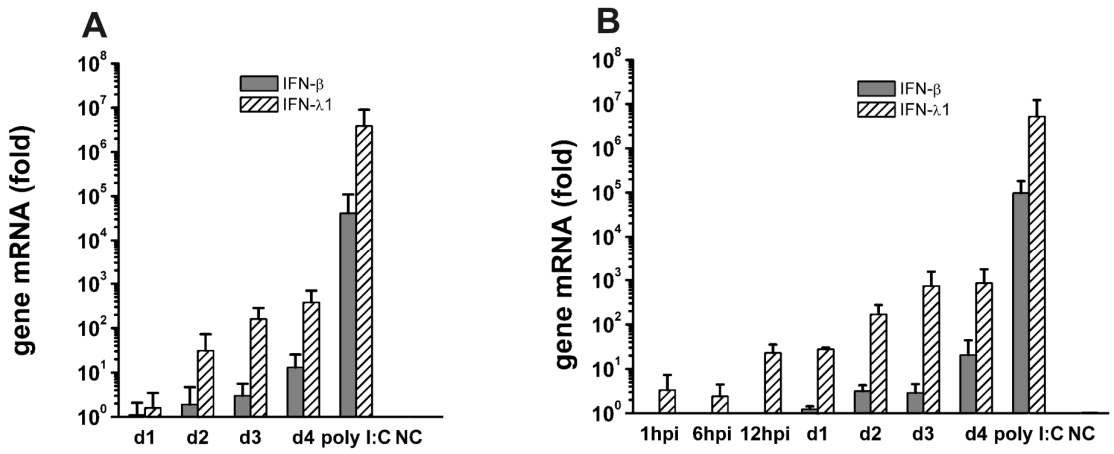

Figure 18: Induction of IFN-ß and IFN-λ1 mRNA expression in A549 cells after GRW/Aa (A) or SANGV (B) infection. A549 cells were infected at MOI 1. Samples were collected at indicated time points. Expression of IFN-ß and IFN-λ1 mRNA were measured by qPCR. Poly I:C, cells transfected at the time of infection with 1.6 µg of poly I:C for six hours. Experiment was performed three times. Data are presented as the mean ± SD of the mean.

A549 cells were infected at MOI 1 with corresponding virus, at indicated time points (Figure 18 A, B) cells were lysed in RLT buffer. RNA was extracted from lysed cells with RNAeasy kit. mRNA expression of IFN-ß and IFN-λ1 was measured by qPCR. The same RNA samples were used before (chapter 4.6.1) to measure MxA mRNA expression after GRW/Aa or SANGV infection of A549 cells.

The expression of IFN-λ1 mRNA was stronger than the expression of IFN-ß mRNA in A549 cells infected with GRW/Aa (Figure 18 A). Interestingly, SANGV induces similar IFN-ß mRNA expression kinetic as GRW/Aa (Figure 18 B). On the other hand, expression of IFN-λ1 mRNA after SANGV infection appeared earlier (at 12 hours post infection) than in cells infected with GRW/Aa (Figure 18 B). Therefore, obtained IFN-ß and IFN-λ1 mRNA kinetics led us to conclude that both interferons play role in MxA induction after infection of A549 cells with either GRW/Aa or SANGV. However, IFN-λ1 could be a primer inducer of MxA since induction of IFN-λ1 mRNA precedes the induction of IFN-ß mRNA (Figure 18).

4.6.3 GRW/Aa and SANGV stocks contain different amounts of IFN-λ1

Very recently Prescott and co-authors revealed that certain hantaviruses are able to induce type III IFNs in type I IFN-deficient Vero E6 cells [78]. This cell line is commonly used for hantavirus stock preparation. Furthermore, infection of HUH7 cell line with a virus stock containing type III IFNs influenced the MxA induction patterns [78].

Therefore, to elucidate whether our virus stocks – which were produced in Vero E6 cells - contain detectable amounts of IFN-λ1 we performed an IFN-λ1-specific ELISA. Vero E6-

derived virus stocks of GRW/Aa, SANGV, HTNV and PHV were UV inactivated before they were evaluated. The IFN-λ1 ELISA revealed that GRW/Aa and HTNV stocks contained very low amounts of IFN-λ1 reaching concentrations of around 100 pg/ml. In contrast, SANGV stocks contained rather high IFN-λ1 concentrations of about 1,750 pg/ml. Comparable concentrations of IFN-λ1 were also found in PHV stocks (Figure 19 A).

To purify viruses from interferons, we precipitated GRW/Aa and SANGV by ultracentrifugation. Vero E6-derived cell culture supernatants were replaced by fresh medium. We observed that the purified GRW/Aa stocks (GRW/Aa-ucf) contained again very low amount of IFN-λ1 comparable with the non-ultracentrifuged virus stocks (Figure 19 A). Purified SANGV stocks (SANGV-ucf), which showed high IFN-λ1 concentration prior purification, contained now very low IFN-λ1 amount as purified and non-purified GRW/Aa stocks (Figure 19 A).

4.6.4 Influence of Vero E6-derived type III IFNs on MxA mRNA induction

To verify the influence of Vero E6-derived IFN-λ1 on obtained MxA protein and mRNA kinetics we performed a function-blocking assay using an anti-IFN-λ1 antibody. To neutralize IFN-λ1 present in Vero E6-prepared stocks, viruses were pre-incubated with blocking anti-IFN-λ1 antibody. Afterwards such pre-treated viruses were added into A549 cells. Cell samples were collected after 16 hours (SANGV) and on the day 4 (GRW/Aa) after infection. These time points were selected according to the strongest MxA mRNA expression detected in previous experiments (Figure 16 and Figure 17). As a control for antibody specificity and blocking efficiency, we pre-incubated in the same way recombinant human IFN-λ1 (rhIFN-λ1) along with anti-IFN-λ1 neutralizing antibody. We observed that anti-IFN-λ1 neutralizing antibody completely inhibits the rhIFN-λ1-mediated MxA response (Figure 19 B, C). As an additional control for antibody specificity and sensitivity, we used recombinant IFN-ß (rhIFN-ß) along with anti-IFN-ß neutralizing antibodies. We observed that although rhIFN-ß itself induces robust MxA responses, the anti-IFN-ß neutralizing antibody inhibited only rhIFN-ß-mediated MxA responses, and not inductions of MxA mediated by GRW/Aa or SANGV stocks containing IFN-λ1. Controls indicated that the anti-IFN antibodies are neutralizing only their homologous targets (Figure 19).

We observed that pretreatment of GRW/Aa stock with neutralizing anti-IFN-λ1 antibody did not influence the MxA mRNA expression (Figure 19 B). However, anti-IFN-λ1 antibody was able to prevent SANGV-mediated MxA mRNA expression (Figure 19 C). Nevertheless, pretreatment of viruses with blocking anti-IFN-ß had no influence on GRW/Aa and SANGV-mediated MxA mRNA expression (Figure 19 B, C).

For additional evidence that the presence of certain amount of Vero E6-derived type III IFNs in virus stocks plays a role in MxA induction, A549 cells were infected with virus stocks purified by ultracentrifugation (ucf). We observed that MxA mRNA expression after 4 days of infection of A549 cells with GRW/Aa-ucf stock was similar to non-ultracentifuged GRW/Aa virus stock (Figure 19 B). This indicates that amount of IFN-λ1 present in Vero E6-prepared GRW/Aa stocks does not influence MxA response after GRW/Aa infection of A549 cells.

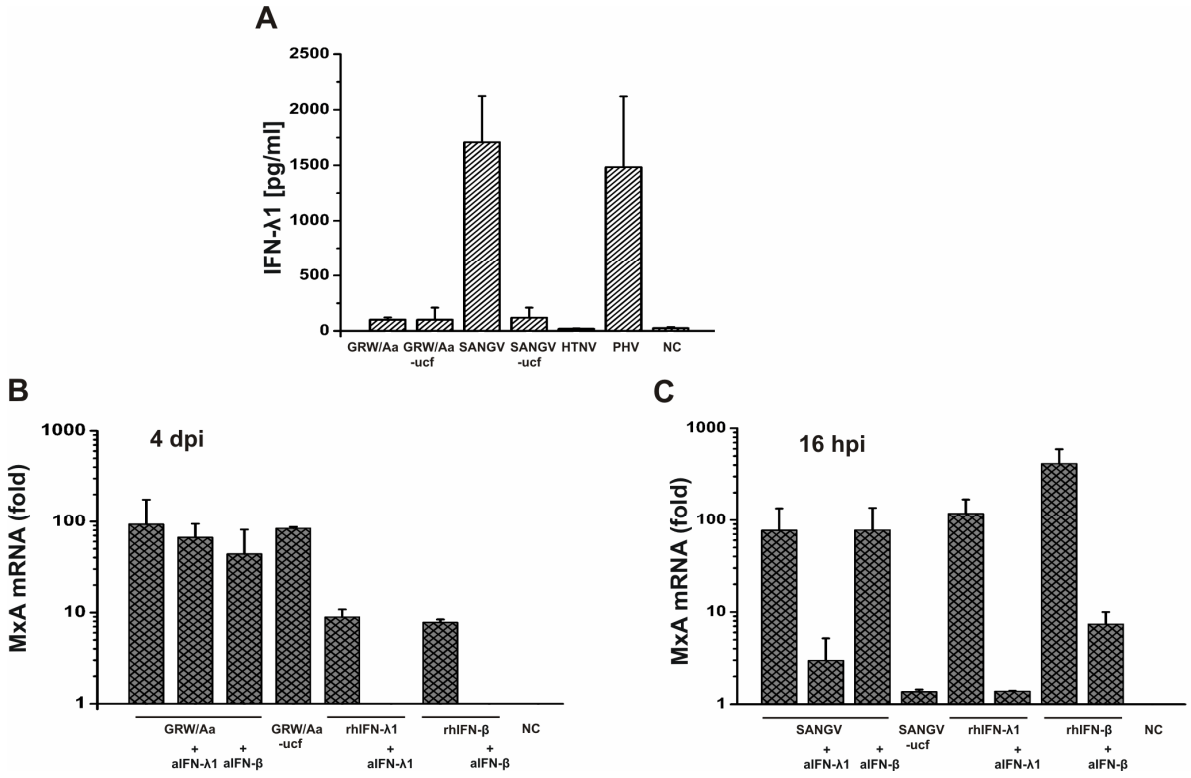

Figure 19: Influence of Vero E6-derived IFN-λ1 on MxA induction in A549 cells infected with GRW/Aa or SANGV. A) Amount of IFN-λ1 present in Vero E6-preapred virus stocks measured by ELISA. NC, negative control. Data are presented as the mean between three independently prepared stocks ± SD from the mean. B) GRW/Aa stocks purified from Vero E6-derived IFN-λ1 (either through function-blocking assay or ultracentrifugation) do not differ from untreated GRW/Aa stocks in their ability to induce MxA expression. C) SANGV stocks purified from Vero E6-derived IFN-λ1 (either through function-blocking assay or ultracentrifugation) differ dramatically from untreated SANGV stocks in their ability to induce MxA expression. MxA mRNA expression was analysed by qPCR and presented as a fold-induction in comparison to untreated A549 cells taken as a negative control (NC). Experiment was performed three times. Data are presented as the mean ± SD of the mean.

In the case of A549 cells infected with purified SANGV stock (SANGV-ucf) we observed remarkable decrease in MxA mRNA expression in comparison to non-ultracentrifuged SANGV stock (Figure 19 C). Thus, we suspect that the observed very early induction of MxA in case of SANGV infection of A549 cells is due to the exogenous type III IFNs, transferred from the Vero E6-prepared virus stocks.

4.6.5 Protein kinase R phosphorylation in response to GRW/Aa and SANGV infection

The role of protein kinase R (PKR) in innate antiviral defense against hantaviruses has not been clearly determined yet. Therefore, we analyzed activation of PKR by GRW/Aa and SANGV.

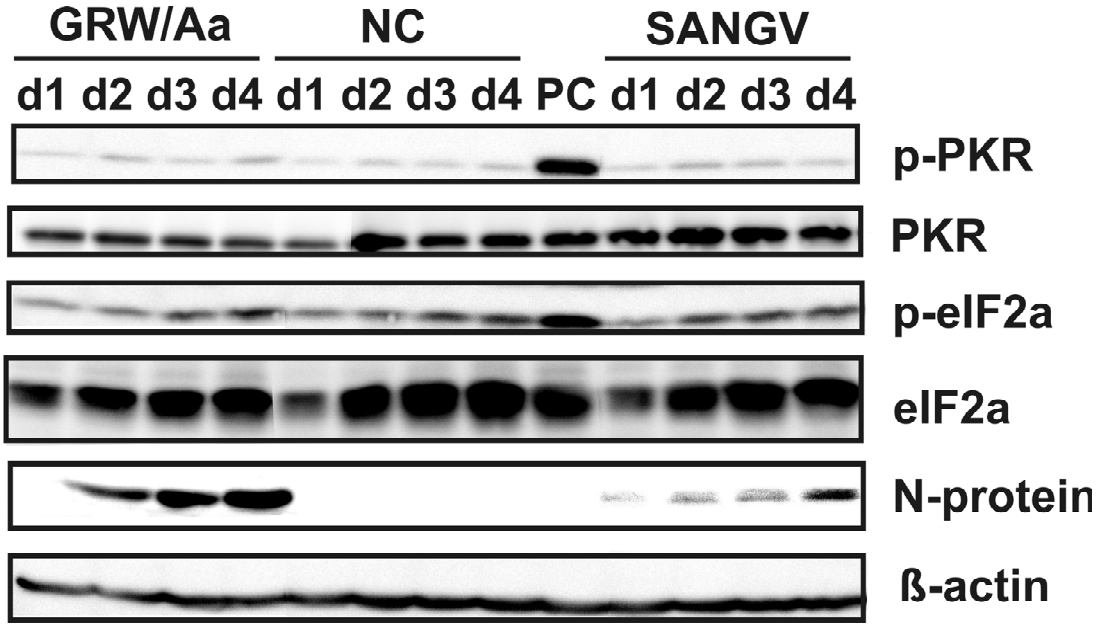

Figure 20: No PKR phosphorylation in response to GRW/Aa and SANGV infection. PC, cells stimulated with poly I:C; NC, cells treated with PBS instead of virus: PKR, protein kinase R; p-PKR, phosphorylated form of PKR; eIF2a, translation initiation factor; p-eIF2a, phosphorylated form of eIF2a; N-protein, viral nucleocapsid protein. β-actin was taken as a reference protein (loading control). Representative results of two independent experiments are shown.

A549 cells were infected with GRW/Aa or SANGV virus at MOI 1, cells were collected at day one, two, three, and four after infection. The phosphorylations of PKR (p-PKR) and its target, the translation initiation factor eIF2a (p-eIF2a), were examined by Western blot (Figure 20). In order to control stabilities of PKR and eIF2a proteins, expression of total PKR and total eIF2a was analyzed by Western blot as well. β-actin was taken as a reference protein (loading control). No difference in phosphorylation of both PKR and eIF2a was observed between infected and control cells, indicating that GRW/Aa as well as SANGV do not activate PKR in the established settings. However, we detected some level of eIF2a phosphorylation at all time points (Figure 20). The phosphorylation patterns of eIF2a were similar for GRW/Aa-infected, SANGV-infected and uninfected A549 cells, indicating that this phosphorylation was not virus-mediated.

Since we did not observe phosphorylation of PKR in response to GRW/Aa or SANGV infection of A549 cells, in the next step we tested the possibility if GRW/Aa or SANGV can inhibit the PKR activation.

Poly I:C is a synthetic dsRNA and serves as a substrate for PKR. Upon the recognition of poly I:C, PKR gets activated and therefore phosphorylated. In a preparatory experiment, the minimum amount of poly I:C needed for PKR activation in A549 cells was found to be 0.5 µg / 1 well (12-well plate format) (Figure 21).

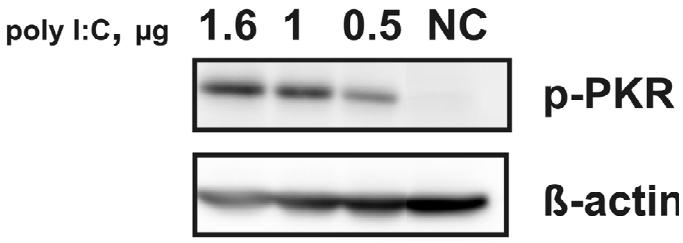

Figure 21: The minimum amount of poly I:C needed for PKR activation. A549 cells were transfected with indicated amount of poly I:C. 6 hours post transfection cells were lysed in protein lysis buffer. The level of PKR phosphorylation (p-PKR) was investigated by Western blot analyses. β-actin was taken as a reference protein (loading control).

The next experiments were designed to investigate if the replicating virus is able to inhibit artificially stimulated (by the transfection of poly I:C) phosphorylation of PKR Therefore, we performed an infection of A549 cells with GRW/Aa or SANGV (MOI 1). After two and four days post infection, the infected cells were transfected with poly I:C in order to stimulate PKR phosphorylation. Six hours post transfection the cells were lysed in lysis buffer and stored at -20ºC until use. The ability of the virus to inhibit stimulated PKR phosphorylation was assessed by Western blot (Figure 22 A and B). Experiments depicted on Figure 22 revealed that both viruses, GRW/Aa and SANGV, are not inhibiting PKR phosphorylation stimulated by poly I:C transfection (Figure 22 A lines 4 and 6 in comparison to control line 2). Even after four days of infection with GRW/Aa or SANGV, the poly I:C stimulated PKR phosphorylation was not inhibited by the replicating viruses (Figure 22 B lines 2 and 4 in comparison to control line 6).

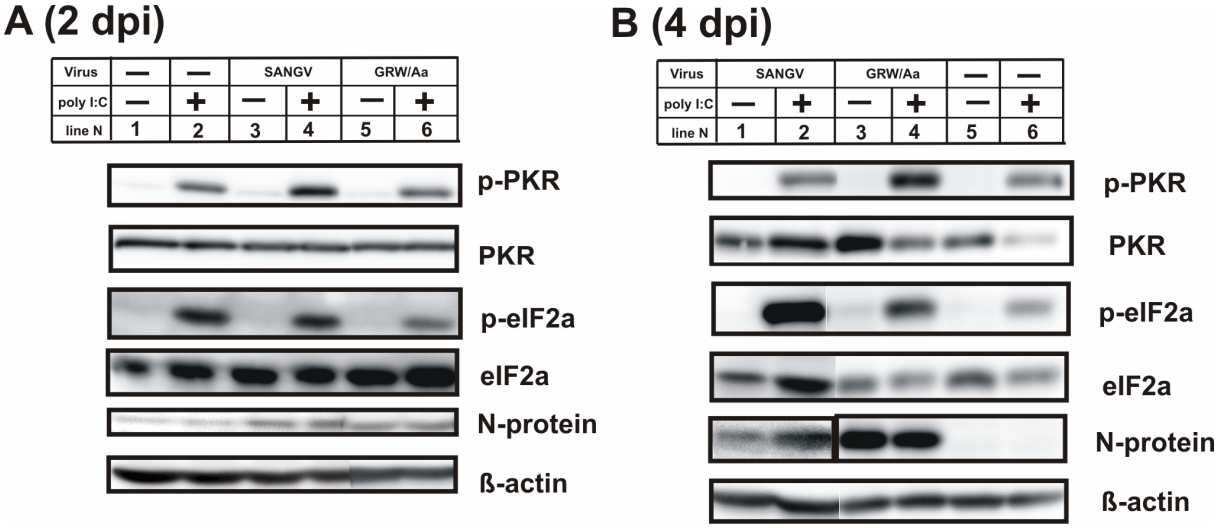

Figure 22: Replicating GRW/Aa or SANGV do not inhibit artificially stimulated phosphorylation of PKR in infected A549 cells. A549 cells were either left untreated (lines 1 and 2, panel A; lines 5 and 6, panel B) or infected with SANGV (lines 3 and 4, panel A; lines 1 and 2, panel B) or infected with GRW/Aa (lines 5 and 6, panel A; lines 3 and 4, panel B) for 2 (A) and 4 (B) days. Then untreated or infected cells were stimulated with poly I:C (lines 2, 4 and 6) for 6 hours, thereafter samples were collected. PKR, protein kinase R; p-PKR, phosphorylated form of PKR; eIF2a, translation initiation factor; p-eIF2a, phosphorylated form of eIF2a; N-protein, viral nucleocapsid protein. β-actin was taken as a reference protein (loading control). Representative results of two independent experiments are shown.

5 Discussion

5.1 Genetic characteristics of the first DOBV isolate from Germany

DOBV-associated HFRS is endemic in North-Eastern Germany. Clinical cases of DOBV-infected humans are regularly diagnosed by serological methods (Robert Koch-Institut: SurvStat, http://www3.rki.de/SurvStat). Important to note that antibodies against DOBV highly cross-react with other hantavirus species (for instance with HTNV), therefore, serodiagnostics are not sensitive enough to finally conclude which virus species had infected a particular patient. However, there is molecular evidence that DOBV infects humans in Germany: one short DOBV-Aa S-segment sequence derived from a patient in Northern Germany has been previously published [100]; other two short DOBV-Aa M- and L-segment sequences were obtained within the current study. Very recently, *A. agrarius* has been reported to be a natural host of DOBV in this particular region although multiple spill-over infections to *A. flavicollis* were observed too [35].

Here we report on cell culture isolation and characterization of the first pathogenic DOBV strain from Germany. The new DOBV isolate was designated as GRW/Aa. Genome sequence and phylogenetic analyses clearly showed that GRW/Aa belongs to the DOBV-Aa lineage (carried by *A. agrarius* mice), although it was found in spill-over infected *A. flavicollis* rodent. To our knowledge, this is a first report on a successful hantavirus cell culture isolation from a spill-over infected animal. Such infections are assumed to be acute and transient, with a higher virus load, and tissues of spill-over infected animals might be even better starting material for virus isolation attempts than tissues of persistently infected natural hosts. Indeed, the virus load in the lungs of the spill-over infected mouse was found to be higher in comparison with lungs of the other two *A. agrarius* mice (trapped in parallel).

DOBV spill-over infections were recently observed to be rather common in Germany [35]. In addition, single DOBV-Af spill-over infection of *A.sylvaticus* and *Mus musculus* has been recently reported [97]. Since hantaviruses have a three-segmented RNA genome, such spill-over infections could lead to the formation of viruses with reassorted genomes, as it has been observed for several orthobunyaviruses [121,122] and for hantaviruses as well [44-46]. In vitro generated reassortants have been observed between SNV and ANDV [123,124] and between SNV and Black Creek Canal virus (BCCV) [125]. Moreover, it has been recently shown that two strains, representing DOBV-Aa and DOBV-Af lineages, could be reassorted in vitro [72]. Nevertheless, the novel GRW/Aa isolate is not a reassorted virus, since our sequence and phylogenetic analyses of complete S-, M- and L-segments did not support any

reassortment events between GRW/Aa genome segments and other hantavirus strains (Table 10, Figure 12).

In addition, we observed the close clustering of GRW/Aa virus sequences with nucleotide sequences amplified from Northern German HFRS patients - H169 and H431 (Figure 14 A, B and C). Thus, all obtained data allowed us to conclude that the GRW/Aa virus could be taken as representative of the pathogenic hantavirus responsible for human infections in this area.

5.2 SANGV, the first hantavirus from Africa

SANGV is a first hantavirus from Africa detected in *Hylomyscus simus* trapped in Guinea, West Africa [14]. A seroepidemiological study based on a combination of screening and confirmatory assays revealed the presence of hantavirus-specific neutralizing antibodies in the average human population in Forest Guinea (seroprevalence 1.2%) and in patients with fever of unknown origin from the same region (seroprevalence 4.4%). Although SANGV-specific IgM and IgG antibodies were detected in one patient who suffered from fever of unknown origin [104], final evidence of SANGV vRNA being present in human specimens has not been obtained. Therefore, SANGV pathogenicity to humans has to be further investigated. We included SANGV in our receptor-blocking studies and investigated SANGV-mediated innate immunity induction patterns in order to estimate its pathogenicity potential.

5.3 GRW/Aa and SANGV utilize distinct cellular receptors in order to maintain virus entry

We identified cellular receptors which are important for GRW/Aa and SANGV entry. Our data revealed that the avß3 integrin and the DAF receptor are utilized by GRW/Aa as entry receptors (Figure 15). Obtained results are in good agreement with the literature and speak for the pathogenicity of GRW/Aa. It has been shown that pathogenic hantaviruses recognize ß3 integrins which play a central role in regulating platelet activation and maintaining vascular permeability [49,52]. DAF has been also demonstrated to be a receptor for pathogenic HTNV and PUUV [55]. It has been reported for coxsackievirus that its attachment to the DAF receptor initiates cytoskeletal rearrangements and opening of the tight junctions allowing the virus to reach its CAR receptor [126]. Nevertheless, utilization of DAF receptor by other hantaviruses has not been assessed yet. We observed that non-pathogenic PHV can be inhibited by anti-DAF antibodies too. Therefore, our findings of PHV entry being efficiently inhibited by anti-DAF antibodies suggest that hantaviruses might use DAF for virus entry regardless their pathogenicity.

However, in the case of SANGV, results of both qPCR and Western blot (Figure 15 A, B) clearly indicated that SANGV infection can be efficiently blocked only by anti-α5ß1 integrin

antibody. Recognition of ß1 integrins by non-pathogenic PHV has been previously shown [49]. Interestingly, although infection by both control viruses (HTNV and PHV) could be efficiently inhibited also by anti-DAF, this was not the case for SANGV which could be inhibited exclusively by ß1-specific antibodies (Figure 15).

The usage of ß1 but not ß3 integrins as entry receptors by SANGV might suggest it being a non-pathogenic virus. However, as it has been mentioned in introduction, pathogenesis of hantaviruses include many processes such as platelets dysfunction, ß3 integrin-mediated dysregulation of endothelial cell barrier, contributions of innate and adaptive immune responses [59,36]. It might turn out that the recognition of ß1 integrin as entry receptor is not a decisive criterion to classify a virus as pathogenic or non-pathogenic. Nevertheless, correlations between SANGV receptor usage and its pathogenicity have to be further characterized.

5.4 Induction of selected innate immunity markers in response to GRW/Aa and SANGV

5.4.1 Induction of antiviral MxA

As a further step towards virus characterization, we investigated the induction of innate immunity markers in response to GRW/Aa and SANGV infection. Since some research groups used A549 and HUH7 cells to study modulation of innate immunity after infection with different hantaviruses, we also used A549 and HUH7 as model cell lines in our study.

We observed no MxA induction (up to day 4 post infection) on protein level in response to GRW/Aa infection of HUH7 cells. However, some basic and continuous expression of MxA mRNA (~ 10 fold induction in comparison to negative control) was detected in HUH7 cells exposed to GRW/Aa infection. Here we speculate that this level of MxA mRNA induction in HUH7 cells might be insufficient to produce an amount of MxA protein detectable by Western blot. Similar results for the absence of MxA protein expression after infection of HUH7 cells with pathogenic HTNV have been previously reported [71].

Given that lung epithelium is one of the main targets during hantavirus infection in humans and A549 cells are established from human lung epithelium, we were further concentrated on studying the induction of innate immunity markers in A549 cells. We observed delayed / late expression of MxA mRNA and protein after infection of A549 cells with GRW/Aa (Figure 16 A, B). On the protein level similar MxA expression kinetics were obtained for HTNV and DOBV-SK/Aa [64,71,72]. Pathogenic hantaviruses could maintain such delayed induction of antiviral responses in order to increase its sufficient replication and dissemination within

tissue, which in turn could cause a prolonged inflammatory response and might contribute to the in vivo virulence [36].

An increase in MxA mRNA expression after SANGV infection of both A549 and HUH7 cell lines was detected already at 6 hours post infection (Figure 17 B, D). In parallel, an early induction of MxA protein expression (day 1 post infection) in response to SANGV infection was observed (Figure 17 A, C). Concerning MxA protein expression, SANGV resembles the behavior of PHV in a cell culture system [71]. Such early induction of antiviral responses might lead to efficient elimination of the virus and could explain the low virus titers in SANGV stocks. However, there was a gap in understanding how the virus induces such an early and strong MxA response in the absence of efficient replication at early time points and why MxA induction patterns stay constant over the time of virus growth (Figure 17 B, D). Therefore, we studied the mechanisms regulating MxA expression and measured induction of type I and III IFNs after SANGV, as well as after GRW/Aa infection.

5.4.2 IFN-β and IFN-λ1 are potential inducers of MxA in A549 cells infected with GRW/Aa and SANGV

It has been reported that pathogenic HTNV does not induce a strong type I IFN (IFN-α/β) response in cell culture [64,76], although "downstream" MxA expression is induced. Until recent time there was no explanation on how MxA can be induced in the absence of type I IFNs. In 2010 it has been shown that certain hantaviruses induce type III IFNs (IFN-λ1, -λ2 and -λ3) in type I IFN deficient Vero E6 cells [78]. Furthermore, Stoltz and Klingström reported that MxA is induced by IFN-λ1 in a type I IFN-independent manner also in A549 cells infected with HTNV [76]. We also detected only a minor induction of type I IFNs on the mRNA level in A549 cells infected with GRW/Aa. Although the induction of IFN-β in A549 infected with GRW/Aa is very low, we cannot completely exclude the role of type I IFNs in GRW/Aa-mediated MxA induction pattern. However, consistent with published studies [76,78], we found a pronounced induction of type III IFNs in response to GRW/Aa infection of A549 cells (Figure 18 A). Evidence that induction of IFN-λ1 mRNA occurred before the induction IFN-ß, strongly suggests that MxA induction is mediated by type III IFNs in GRW/Aa infected A549 cells.

We conclude that observed MxA expression patterns are due to de novo synthesized type III IFNs induced by the virus infection and not due to exogenous IFN-λ1 which was found in the Vero E6-prepared virus stock at a barely detectable amount. Following observations underline this conclusion:

First, induction of INF-λ1 occurred along with the intracellular replication of GRW/Aa.

Second, Vero E6-prepared GRW/Aa virus stocks contain only low level of IFN-λ1 (Figure 19 A), and this amount of IFN-λ1 was experimentally shown to be unable to induce MxA expression in A549 (data not shown).
Third, pre-incubation of GRW/Aa virus stock with neutralizing anti-IFN-λ1 antibody did not influence MxA mRNA induction in response to GRW/Aa infection (Figure 19 B).
Finally, the stock of GRW/Aa purified by ultracentrifugation induced the same level of MxA induction as the non-purified stock (Figure 19 B).
However, in contrast to GRW/Aa, we found SANGV to be a good inducer of type III IFNs in type I IFN deficient Vero E6 cells (Figure 19 A). We were able to block MxA induction in A549 cells infected with a SANGV stock which was treated with the neutralizing anti-IFN-λ antibody. Moreover, we showed that a type III IFNs free SANGV stock does not induce an early MxA mRNA induction in A549 cells (Figure 19 C). Therefore, we suspect that observed early MxA induction in A549 cells infected with SANGV are due to exogenous type III IFNs, transferred from a Vero E6-prepared stock.
The experience with SANGV stocks shows that in order to investigate the real virus-mediated induction of innate immunity, hantavirus stocks free of cytokines are needed. As shown by us, ultracentrifugation procedure offers a good tool for the purification of virus stocks.

5.4.3 Influence of GRW/Aa and SANGV on protein kinase R (PKR) activity

The important role of PKR in antiviral defense has been shown for many human viruses such as herpesviruses, poxviruses, influenza viruses, human immunodeficiency virus-1, hepatitis C virus and others [79,127]. These viruses utilize a number of strategies to counteract dsRNA-dependent pathways to avoid the deleterious effects of the PKR. There are viral proteins that interfere with these pathways at different levels, by inhibiting PKR activation, sequestering dsRNA, inhibiting PKR dimerization, synthesizing PKR pseudosubstrates, activating antagonist phosphatases, or degrading PKR. For example, NS1 protein of influenza A (A/NS1) virus has been reported to interact directly with PKR, inhibiting its activity [128]. It has been also postulated that A/NS1 is sequestering dsRNA from PKR recognition. However, very few studies were so far reported which would analyze hantavirus-mediated PKR activation. Therefore, we performed experiments to study GRW/Aa interaction with PKR.
We observed no PKR activation (phosphorylation) after infection of A549 cells with GRW/Aa or SANGV (Figure 20). One possible explanation could be that hantaviruses, in our case GRW/Aa and SANGV, evolved mechanisms to inhibit PKR activity. We performed PKR inhibition assay to investigate the ability of GRW/Aa and SANGV to inhibit artificially stimulated PKR activity (Figure 22 A, B). In our experimental settings, we failed to observe

such inhibition of artificially stimulated PKR by GRW/Aa as well as by SANGV. Nevertheless, a hantavirus-mediated inhibition of PKR still cannot be completely excluded, since there are many other mechanisms regulating PKR activity which effects cannot be evaluated in our experimental settings. For example, the most relevant explanation why we did not see inhibition of PKR by GRW/Aa and SANGV is that viruses sequester only their own virus-derived dsRNA, but not synthetic analogs of dsRNA. That means that hantaviruses do not recognize poly I:C as a dsRNA and consequently do not prevent poly I:C mediated stimulation of PKR. Such mechanism of sequestering of dsRNA has been proposed and discussed for influenza A-maintained inhibition of PKR activity [79,129,130].

Nevertheless, PKR induction and inhibition patterns observed in the present study allow us to conclude that GRW/Aa as well as SANGV infections neither activate PKR nor inhibit artificially stimulated PKR phosphorylation in our experimental settings.

Availability of functional reverse genetics for hantaviruses would be a perfect tool in further characterization of functional interactions between hantaviruses and PKR. For example, it would be possible to study whether mutated hantavirus (lacking functional domains in nucleocapsid protein or/and viral polymerase) alters PKR activity as it was shown for influenza B virus recombinant mutants lacking complete NS1 protein or expressing its truncated forms [82]. At the moment no functional reverse genetic system is available for hantaviruses, which needs to be established to allow further progress.

5.5 Hantaviruses and interferon induction

The in vitro modulation of innate immunity by pathogenic and non-pathogenic hantaviruses seems not to be conclusively associated with virus pathogenesis. Contradictory results have been published, making it difficult to distinguish the behavior of pathogenic from non-pathogenic virus in a cell culture system. There is a study demonstrating that pathogenic HTNV clearly induced the production of IFN-ß, whereas expression of this cytokine was barely detectable in the supernatant or in extracts from cells infected with low-pathogenic TULV. However, human endothelial cells infected with TULV start to express the antiviral MxA protein 34 hours earlier than HTNV infected cells [64]. Another work showed that overall cellular transcriptional responses were more altered by pathogenic SNV compared to non-pathogenic PHV [65]. Other research groups have observed major differences in the early interferon responses between pathogenic New York-1 virus (NY-1V), HTNV, Andes virus (ANDV) and non-pathogenic PHV hantavirus [67,68]. Moreover, a recent study has reported that inhibition of early IFN responses is necessary but alone insufficient for a hantavirus to be pathogenic, since the expression of TULV Gn protein cytoplasmic tail (Gn-T) regulates IFN

induction in similar way as pathogenic NY-1V, ANDV, and HTNV [131]. In summary, reported difficulties suggest that hantavirus pathogenesis is a complex process that includes not only contributions from immune responses (immune complexes, complement activation, cytotoxic T cells, etc.), but is also based on platelet dysfunction and the dysregulation of endothelial cell barrier functions. Therefore, availability of an animal model mimicking human hantavirus disease would be a perfect tool for the characterization of virulence executed by different hantaviruses. However, only one hamster model, imitating ANDV caused illness of humans, is described so far [132,133]. This model was used for the study of pathogenicity determinants of ANDV. The authors generated an in vitro reassortant virus containing S- and L-segments from SNV and the M-segment from ANDV. This reassortant virus elicited high titers and ANDV-specific neutralizing antibodies in infected hamsters. However, the infected animals did not show signs of HPS disease and the infection was not lethal, indicating that the M-segment alone is not sufficient to cause the disease [123].

6 Conclusion

Table 12: Molecular characteristics and pathogenicity potential of GRW/Aa from Germany and Sangassou virus from Africa

	GRW/Aa	SANGV
virus species	DOBV-Aa	SANGV
reservoir host	rodents (family *Muridae*, subfamily *Murinae*) *Apodemus agrarius*	rodents (family *Muridae*, subfamily *Murinae*) *Hylomyscus simus*
spill-over reservoir host	*Apodemus flavicollis*	unknown
geographical distribution	Europe (north of Germany)	Africa (Guinea)
genome S-segment (nt) M-segment (nt) L-segment (nt)	 1,675 3,644 6,532	 1,746 * 3,650 * 6,531 *
panhandle structure (bp)	22-29	17-19 *
sign of intragenic recombination or reassortment in phylogenetic analyses	no	no *
serological proof of human infections	yes	yes **
patient-derived sequence	yes	no
cellular receptor (Vero E6)	β3 integrins, DAF	β1 integrins
induction of type III IFNs (Vero E6)	moderate	strong
induction of type I IFNs (A549)	moderate	moderate
induction of type III IFNs (A549)	delayed (2 dpi)	early (16 hpi)
induction of MxA mRNA (A549)	late (3 dpi)	early (6 hpi)
influence of Vero E6-derived type III IFNs on observed MxA induction	no	strong
induction of PKR phosphorylation (A549)	no	no
inhibition of poly I:C stimulated PKR phosphorylation	no	no
human disease	HFRS	?

* Klempa B., Witkowski P.T., Popugaeva E., Auste B., Koivogui L., Fichet-Calvet E., Meulen J., and Kruger D.H. (2011) Sangassou virus, the first hantavirus from Africa, displays distinct genetic and functional properties in the group of Murinae-associated hantaviruses. J Virol in revision.
** [104]

In summary, the current study presents molecular characteristics of two novel hantaviruses: GRW/Aa and SANGV. Based on these characteristics we tried to estimate the pathogenicity

potential of GRW/Aa and SANGV. Both viruses are members of *Murinae*-associated hantaviruses, however, GRW/Aa and SANGV exhibit completely distinct pathogenicity determinants in cell culture systems. As it was expected, GRW/Aa demonstrates properties of pathogenic hantaviruses. It recognizes β3 integrins as entry receptors in addition to DAF and induces late expression of MxA and type III IFNs. The final proof of GRW/Aa pathogenicity in humans was shown by phylogenetic analyses, where sequences from the GRW/Aa isolate cluster together with patient-derived sequences from Germany.

Concerning SANGV, it displays unique in vitro properties. It recognizes β1 integrins as entry receptors, being the first virus not using DAF, and induces a strong type III IFNs response in Vero E6 cells. Whether these characteristics have some consequences for the SANGV pathogenicity remains to be answered. Nevertheless, properties observed within the current study make GRW/Aa and SANGV useful to be included in comparative studies focusing on hantavirus pathogenesis.

7 References

1. Lee HW, Lee PW, Johnson KM (1978) Isolation of the etiologic agent of Korean hemorrhagic fever. J Infect Dis 137: 298–308.
2. Krüger DH, Ulrich R, Lundkvist Å (2001) Hantavirus infections and their prevention. Microbes Infect 3: 1129-1144.
3. LeDuc J, Childs J, Glass G (1992) The hantaviruses, etiologic agents of hemorrhagic fever with renal syndrome: a possible cause of hypertension and chronic renal disease in the United States. Annu Rev Publ Health 13: 79–98.
4. Casals J, Henderson BE, Hoogstraal H, Johnson KM, Shelokov A (1970) A review of Soviet viral hemorrhagic fevers, 1969. J Infect Dis 122: 437-453.
5. Cohen M (1982) Epidemic hemorrhagic fever revisited. Rev Infect Dis 4: 992-997.
6. French GR, Foulke RS, Brand OA, Eddy GA, Lee HW, et al. (1981) Korean hemorrhagic fever: propagation of the etiologic agent in a cell line of human origin. Science 211: 1046.
7. Brummer-Korvenkontio M, Vaheri A, Hovi T, Bonsdorff CH von, Vuorimies J, et al. (1980) Nephropathia epidemica: detection of antigen in bank voles and serologic diagnosis of human infection. J Infect Dis 141: 131-134.
8. Lee HW, Baek LJ, Johnson KM (1982) Isolation of Hantaan virus, the etiologic agent of Korean hemorrhagic fever, from wild urban rats. J Infect Dis 146: 638-644.
9. Avsic-Zupanc T, Xiao SY, Stojanovic R, Gligic A, Groen G van der, et al. (1992) Characterization of Dobrava virus: a hantavirus from Slovenia, Yugoslavia. J Med Virol 38: 132-137.
10. Nichol S, Spiropoulou C, Morzunov S, Rollin P, Ksiazek T, et al. (1993) Genetic identification of a hantavirus associated with an outbreak of acute respiratory illness. Science 262: 914-917.
11. Song J-W, Baek L-J, Gajdusek, D Carleton Yanagihara R, Gavrilovskaya I, Luft BJ, et al. (1994) Isolation of pathogenic hantavirus from white-footed mouse (Peromyscus leucopus). Lancet 344: 1637.
12. Calderón G, Pini N, Bolpe J, Levis S, Mills J, et al. (1999) Hantavirus reservoir hosts associated with peridomestic habitats in Argentina. Emerg Infect Dis 5: 792-797.
13. Lee PW, Amyx HL, Yanagihara R, Gajdusek DC, Goldgaber D, et al. (1985) Partial characterization of Prospect Hill virus isolated from meadow voles in the United States. J Infect Dis 152: 826–829.
14. Klempa B, Fichet-Calvet E, Lecompte E (2006) Hantavirus in African wood mouse, Guinea. Emerg Infect Dis 12: 838-840.
15. Klempa B, Fichet-Calvet E, Lecompte E, Auste B, Aniskin V, et al. (2007) Novel hantavirus sequences in shrew, Guinea. Emerg Infect Dis 13: 520-522.
16. Kang HJ, Kadjo B, Dubey S, Jacquet F, Yanagihara R (2011) Molecular evolution of Azagny virus, a newfound hantavirus harbored by the West African pygmy shrew (Crocidura obscurior) in Cote d'Ivoire. Virology J 8: 373.

17. Kang HJ, Arai S, Hope AG, Cook J a, Yanagihara R (2010) Novel hantavirus in the flat-skulled shrew (Sorex roboratus). Vector Borne Zoonot Dis 10: 593-597.

18. Arai S, Song J-W, Sumibcay L, Bennett SN, Nerurkar VR, et al. (2007) Hantavirus in northern short-tailed shrew, United States. Emerg Infect Dis 13: 1420-1423.

19. Song J-W, Kang H, Song K (2007) Newfound hantavirus in Chinese mole shrew, Vietnam. Emerg Infect Dis 13: 1784-1787.

20. Song J-W, Gu SH, Bennett SN, Arai S, Puorger M, et al. (2007) Seewis virus, a genetically distinct hantavirus in the Eurasian common shrew (Sorex araneus). Virology J 4: 114.

21. Arai S, Bennett SN, Sumibcay L, Cook JA, Song JW, et al. (2008) Phylogenetically distinct hantaviruses in the masked shrew (Sorex cinereus) and dusky shrew (Sorex monticolus) in the United States. Am J Trop Med Hyg 78: 348-351.

22. Song J-W, Kang HJ, Gu SH, Moon SS, Bennett SN, et al. (2009) Characterization of Imjin virus , a newly isolated hantavirus from the Ussuri white-toothed shrew (Crocidura lasiura). J Virol 83: 6184-6191.

23. Arai S, Ohdachi SD, Asakawa M, Kang HJ, Mocz G, et al. (2008) Molecular phylogeny of a newfound hantavirus in the Japanese shrew mole (Urotrichus talpoides). Proc Natl Acad Sci U S A 105: 16296-16301.

24. Kang HJ, Bennett SN, Dizney L, Sumibcay L, Arai S, et al. (2009) Host switch during evolution of a genetically distinct hantavirus in the American shrew mole (Neurotrichus gibbsii). Virology 388: 8–14.

25. Kang HJ, Bennett SN, Hope AG, Cook J a, Yanagihara R (2011) Shared ancestry between a newfound mole-borne hantavirus and hantaviruses harbored by Cricetid rodents. J Virol 85: 7496-7503.

26. Plyusnin A (2002) Genetics of hantaviruses: implications to taxonomy. Arch Virol 147: 665-682.

27. Kukkonen SKJ, Vaheri A, Plyusnin A (2005) L protein, the RNA-dependent RNA polymerase of hantaviruses. Arch Virol 150: 533-556.

28. Garcin D, Lezzi M, Dobbs M, Elliott RM, Schmaljohn C, et al. (1995) The 5’ ends of Hantaan virus (Bunyaviridae) RNAs suggest a prime-and-realign mechanism for the initiation of RNA synthesis. J Virol 69: 5754-5762.

29. Mir MA, Sheema S, Haseeb A, Haque A (2010) Hantavirus nucleocapsid protein has distinct m7G cap- and RNA-binding sites. J Biol Chem 285: 11357-11368.

30. Jonsson CB, Schmaljohn CS (2001) The replication pathway. In: Hantaviruses. Springer. pp. 24-28.

31. Abraham G, Pattnaik AK (1983) Early RNA synthesis in Bunyamwera virus-infected cells. J Gen Virol 64: 1277-1290.

32. Patterson JL, Kolakofsky D (1984) Characterization of La Crosse virus small-genome transcripts. J Virol 49: 680-685.

33. Muranyi W, Bahr U, Zeier M, Woude FJ van der (2005) Hantavirus infection. J Am Soc Nephrol 16: 3669-79.

34. Jackson AP, Charleston MA (2004) A cophylogenetic perspective of RNA-virus evolution. Mol Biol Evol 21: 45-57.

35. Schlegel M, Klempa B, Auste B, Bemmann M, Schmidt-Chanasit J, et al. (2009) Dobrava-Belgrade virus spillover infections, Germany. Emerg Infect Dis 15: 2017-2020.

36. Schönrich G, Rang A, Lütteke N, Raftery MJ, Charbonnel N, et al. (2008) Hantavirus-induced immunity in rodent reservoirs and humans. Immunol Rev 225: 163-189.

37. Krüger DH, Schönrich G, Klempa B (2011) Human pathogenic hantaviruses and prevention of infection. Hum Vaccin 7: 685-693.

38. Easterbrook JD, Klein SL (2008) Immunological mechanisms mediating hantavirus persistence in rodent reservoirs. PLoS pathogens 4: e1000172.

39. Plyusnin A, Vapalahti O, Vaheri A (1996) Hantaviruses: genome structure, expression and evolution. J Gen Virol 77: 2677-2687.

40. Ramsden C, Holmes EC, Charleston MA (2009) Hantavirus evolution in relation to its rodent and insectivore hosts: no evidence for codivergence. Mol Biol Evol 26: 143-153.

41. Ramsden C, Melo FL, Figueiredo LM, Holmes EC, Zanotto PM a (2008) High rates of molecular evolution in hantaviruses. Mol Biol Evol 25: 1488-1492.

42. Jonsson CB, Figueiredo LTM, Vapalahti O (2010) A global perspective on hantavirus ecology, epidemiology, and disease. Clin Microbiol Rev 23: 412-441.

43. Klempa B, Schmidt HA, Ulrich R, Kaluz S, Labuda M, et al. (2003) Genetic interaction between distinct Dobrava hantavirus subtypes in Apodemus agrarius and A. flavicollis in nature. J Virol 77: 804-809.

44. Li D, Schmaljohn AL, Anderson K, Schmaljohn CS (1995) Complete nucleotide sequences of the M and S segments of two hantavirus isolates from California: evidence for reassortment in nature among viruses related to hantavirus pulmonary. Virology: 973-983.

45. Zou Y, Hu J, Wang ZX, Wang DM, Yu C, et al. (2008) Genetic characterization of hantaviruses isolated from Guizhou, China: evidence for spillover and reassortment in nature. Jo Med Virol 80: 1033–1041.

46. Razzauti M, Plyusnina A, Sironen T, Henttonen H, Plyusnin A (2009) Analysis of Puumala hantavirus in a bank vole population in northern Finland: evidence for co-circulation of two genetic lineages and frequent reassortment between strains. J Gen Virol 90: 1923-1931.

47. Song J-W, Baek LJ, Schmaljohn CS, Yanagihara R (2007) Thottapalayam virus, a prototype shrewborne hantavirus. Emerg Infect Dis 13: 980-985.

48. Yadav PD, Vincent MJ, Nichol ST (2007) Thottapalayam virus is genetically distant to the rodent-borne hantaviruses, consistent with its isolation from the Asian house shrew (Suncus murinus). Virology J 4: 80.

49. Gavrilovskaya IN, Shepley M, Shaw R, Ginsberg MH, Mackow ER (1998) beta3 Integrins mediate the cellular entry of hantaviruses that cause respiratory failure. Proc Natl Acad Sci U S A 95: 7074-7079.

50. Stewart PL, Nemerow GR (2007) Cell integrins: commonly used receptors for diverse viral pathogens. Trends Microbiol 15: 500-507.

51. Gahmberg CG, Fagerholm SC, Nurmi SM, Chavakis T, Marchesan S, et al. (2009) Regulation of integrin activity and signalling. Biochim Biophys Acta 1790: 431-44.

52. Gavrilovskaya IN, Brown EJ, Ginsberg MH, Mackow ER (1999) Cellular entry of hantaviruses which cause hemorrhagic fever with renal syndrome is mediated by beta 3 integrins. J Virol 73: 3951-3959.

53. Gavrilovskaya IN, Peresleni T, Geimonen E, Mackow ER (2002) Pathogenic hantaviruses selectively inhibit beta3 integrin directed endothelial cell migration. Arch Virol 147: 1913-1931.

54. Matthys VS, Gorbunova EE, Gavrilovskaya IN, Mackow ER (2009) Andes Virus Recognition of Human and Syrian Hamster 3 Integrins Is Determined by an L33P Substitution in the PSI Domain. J Virol 84: 352-360.

55. Krautkramer E, Zeier M (2008) Hantavirus causing hemorrhagic fever with renal syndrome enters from the apical surface and requires Decay-Accelerating Factor (DAF/CD55). J Virol 82: 4257-4264.

56. Choi Y, Kwon Y, Kim S, Park J, Lee K, et al. (2008) A hantavirus causing hemorrhagic fever with renal syndrome requires gC1qR/p32 for efficient cell binding and infection. Virology 381: 178-183.

57. Feng X, Tonnesen MG, Peerschke EIB, Ghebrehiwet B (2002) Cooperation of C1q receptors and integrins in C1q-mediated endothelial cell adhesion and spreading. J Immunol 168: 2441-2448.

58. Raymond T, Gorbunova E, Gavrilovskaya IN, Mackow ER (2005) Pathogenic hantaviruses bind plexin-semaphorin-integrin domains present at the apex of inactive, bent alphavbeta3 integrin conformers. Proc Natl Acad Sci U S A 102: 1163-1168.

59. Mackow ER, Gavrilovskaya IN (2009) Hantavirus regulation of endothelial cell functions. Thromb Haemost 102: 1030-1041.

60. Cosgriff TM, Lee HW, See AF, Parrish DB, Moon JS, et al. (1991) Platelet dysfunction contributes to the haemostatic defect in haemorrhagic fever with renal syndrome. Trans R Soc Trop Med Hyg 85: 660–663.

61. Donnelly RP, Kotenko SV (2010) Interferon-lambda: a new addition to an old family. J Interferon Cytokine Res 30: 555-564.

62. Katze MG, He Y, Gale M (2002) Viruses and interferon: a fight for supremacy. Nature Rev Immunol 2: 675-687.

63. Hengel H, Koszinowski UH, Conzelmann K-K (2005) Viruses know it all: new insights into IFN networks. Trends Immunol 26: 396-401.

64. Kraus AA, Raftery MJ, Giese T, Ulrich R, Zawatzky R, et al. (2004) Differential antiviral response of endothelial cells after infection with pathogenic and nonpathogenic hantaviruses. J Virol 78: 6143-6150.

65. Khaiboullina SF, Rizvanov AA, Otteson E, Miyazato A, Maciejewski J, et al. (2004) Regulation of cellular gene expression in endothelial cells by Sin Nombre and Prospect Hill viruses. Viral Immunol 17: 234-251.

66. Geimonen E, Neff S, Raymond T, Kocer SS, Gavrilovskaya IN, et al. (2002) Pathogenic and nonpathogenic hantaviruses differentially regulate endothelial cell responses. Proc Natl Acad Sci U S A 99: 13837-13842.

67. Alff PJ, Gavrilovskaya IN, Gorbunova E, Endriss K, Chong Y, et al. (2006) The pathogenic NY-1 hantavirus G1 cytoplasmic tail inhibits RIG-I- and TBK-1-directed interferon responses. J Virol 80: 9676-9686.

68. Spiropoulou CF, Albariño CG, Ksiazek TG, Rollin PE (2007) Andes and Prospect Hill hantaviruses differ in early induction of interferon although both can downregulate interferon signaling. J Virol 81: 2769-2776.

69. Nam J-H, Hwang K-A, Yu C-H, Kang T-H, Shin J-Y, et al. (2003) Expression of interferon inducible genes following Hantaan virus infection as a mechanism of resistance in A549 cells. Virus Genes 26: 31–38.

70. Prescott J, Ye C, Sen G, Hjelle B (2005) Induction of innate immune response genes by Sin Nombre hantavirus does not require viral replication. J Virol 79: 15007-15015.

71. Handke W, Oelschlegel R, Franke R, Krüger DH, Rang A (2009) Hantaan virus triggers TLR3-dependent innate immune responses. J Immunol 182: 2849-2858.

72. Kirsanovs S, Klempa B, Franke R, Lee M-H, Schönrich G, et al. (2010) Genetic reassortment between high-virulent and low-virulent Dobrava-Belgrade virus strains. Virus Genes 41: 319-328.

73. Haller O, Kochs G (2011) Human MxA protein: an interferon-induced dynamin-like GTPase with broad antiviral activity. J Interferon Cytokine Res 31: 79-87.

74. Kanerva M, Melén K, Vaheri A, Julkunen I (1996) Inhibition of Puumala and Tula hantaviruses in Vero cells by MxA protein. Virology 224: 55-62.

75. Frese M, Kochs G, Feldmann H, Hertkorn C, Haller O (1996) Inhibition of bunyaviruses, phleboviruses, and hantaviruses by human MxA protein. J Virol 70: 915-923.

76. Stoltz M, Klingström J (2010) Alpha/beta interferon (IFN-alpha/beta)-independent induction of IFN-lambda1 (interleukin-29) in response to Hantaan virus Infection. J Virol 84: 9140-9148.

77. Holzinger D, Jorns C, Stertz S, Boisson-Dupuis S, Thimme R, et al. (2007) Induction of MxA gene expression by Influenza A virus requires type I or type III interferon signaling. J Virol 81: 7776-7785.

78. Prescott J, Hall P, Acuna-Retamar M, Ye C, Wathelet MG, et al. (2010) New World hantaviruses activate IFNlambda production in type I IFN-deficient vero E6 cells. PloS one 5: e11159.

79. García MA, Gil J, Ventoso I, Guerra S, Domingo E, et al. (2006) Impact of protein kinase PKR in cell biology: from antiviral to antiproliferative action. Microbiol Mol Biol Rev 70: 1032-1060.

80. Pindel A, Sadler A (2011) The role of protein kinase R in the interferon response. J Interferon Cytokine Res 31: 59-70.

81. García MA, Meurs EF, Esteban M (2007) The dsRNA protein kinase PKR: virus and cell control. Biochimie 89: 799-811.

82. Dauber B, Schneider J, Wolff T (2006) Double-stranded RNA binding of influenza B virus nonstructural NS1 protein inhibits protein kinase R but is not essential to antagonize production of Alpha/Beta interferon. J Virol 80: 11667-11677.

83. Ikegami T, Narayanan K, Won S, Kamitani W, Peters CJ, et al. (2009) Rift Valley fever virus NSs protein promotes post-transcriptional downregulation of protein kinase PKR and inhibits eIF2alpha phosphorylation. PLoS pathogens 5: e1000287.

84. Hofmann J, Meisel H, Klempa B, Vesenbeckh, Silvan M. Beck R, Michel D, et al. (2008) Hantavirus outbreak, Germany, 2007. Emerg Infect Dis 14: 850-852.

85. Tersago K, Verhagen R, Vapalahti O, Heyman P, Ducoffre G, et al. (2011) Hantavirus outbreak in Western Europe: reservoir host infection dynamics related to human disease patterns. Epidemiol Infect 139: 381-390.

86. Faber MS, Ulrich RG, Frank C, Brockmann SO, Pfaff GM, et al. (2010) Steep rise in notified hantavirus infections in Germany, April 2010. Euro Surveill 15: 19574.

87. Ulrich RG, Schmidt-Chanasit J, Schlegel M, Jacob J, Pelz H-J, et al. (2008) Network "Rodent-borne pathogens" in Germany: longitudinal studies on the geographical distribution and prevalence of hantavirus infections. Parasitol Res 103: S121-S129.

88. Meisel H, Lundkvist, Gantzer K (1998) First case of infection with hantavirus Dobrava in Germany. Eur J Clin Microbiol Infect Dis: 884-885.

89. Mertens M, Wölfel R, Ullrich K, Yoshimatsu K, Blumhardt J, et al. (2009) Seroepidemiological study in a Puumala virus outbreak area in South-East Germany. Med Microbiol Immunol 198: 83-91.

90. Klempa B, Meisel H, Ra S, Bartel J, Ulrich R, et al. (2003) Occurrence of renal and pulmonary syndrome in a region of Northeast Germany where Tula hantavirus circulates. J Clin Microbiol 41: 4894-4897.

91. Avsic-Zupanc T, Petrovec M, Furlan P, Kaps R, Elgh F, et al. (1999) Hemorrhagic fever with renal syndrome in the Dolenjska region of Slovenia-a 10-year survey. Clin Infect Dis 28: 860-865.

92. Papa A, Antoniadis A (2001) Hantavirus infections in Greece-an update. Eur J Epidemiol 17: 189-194.

93. Klempa B, Stanko M, Labuda M, Ulrich R, Meisel H, et al. (2005) Central European Dobrava hantavirus isolate from a striped field mouse (Apodemus agrarius). J Clin Microbiol 43: 2756-2763.

94. Klempa B, Tkachenko EA, Dzagurova TK, Yunicheva YV, Morozov VG, et al. (2008) Hemorrhagic fever with renal syndrome caused by 2 lineages of Dobrava hantavirus, Russia. Emerg Infect Dis 14: 617-625.

95. Nemirov K, Vapalahti O, Lundkvist A, Vasilenko V, Golovljova I, et al. (1999) Isolation and characterization of Dobrava hantavirus carried by the striped field mouse (Apodemus agrarius) in Estonia. J Gen Virol 80: 371-379.

96. Dzagurova TK, Witkowski PT, Tkachenko EA, Klempa B, Morozov VG, et al. (2011) Isolation of Sochi virus from a fatal case of hantavirus disease with fulminant clinical course. Clin Infect Dis: in press.

97. Weidmann M, Schmidt P, Vackova M, Krivanec K, Munclinger P, et al. (2005) Identification of genetic evidence for Dobrava virus spillover in rodents by nested reverse transcription (RT)-PCR and TaqMan RT-PCR. J Clin Microbiol 43: 808-812.

98. Kruger DH, Klempa B (2011) Dobrava-Belgrade Virus. In: Liu D, editor. Molecular detection of human viral pathogens. Boca Raton: CRC Press. pp. 631-636.

99. Schütt M, Meisel H, Krüger DH, Ulrich R, Dalhoff K, et al. (2004) Life-threatening Dobrava hantavirus infection with unusually extended pulmonary involvement. Clin Nephrol 62: 54-57.

100. Klempa B, Schuett M, Auste B, Labuda M, Ulrich R, et al. (2004) First molecular identification of human Dobrava virus infection in Central Europe. J Clin Microbiol 42: 1322-1325.

101. Sibold C, Ulrich R, Labuda M, Lundkvist A, Martens H, et al. (2001) Dobrava hantavirus causes hemorrhagic fever with renal syndrome in central Europe and is carried by two different Apodemus mice species. J Med Virol 63: 158-167.

102. Gonzalez JP, Josse R, Johnson E, Merlin M, Georges A, et al. (1989) Antibody prevalence against haemorrhagic fever viruses in randomized representative Central African populations. Res Virol 140: 319–331.

103. Botros BA, Sobh M, Wierzba T, Arthur RR, Mohareb EW, et al. (2004) Prevalence of hantavirus antibody in patients with chronic renal disease in Egypt. Trans R Soc Trop Med Hyg 98: 331-336.

104. Klempa B, Koivogui L, Sylla O, Koulemou K, Auste B, et al. (2010) Serological evidence of human hantavirus infections in Guinea, West Africa. J Infect Dis 201: 1031-1034.

105. Kraus AA, Priemer C, Heider H, Krüger DH, Ulrich R (2005) Inactivation of Hantaan virus-containing samples for subsequent investigations outside biosafety level 3 facilities. Intervirology 48: 255-261.

106. Heider H, Ziaja B, Priemer C, Lundkvist A, Neyts J, et al. (2001) A chemiluminescence detection method of hantaviral antigens in neutralisation assays and inhibitor studies. J Virol Methods 96: 17-23.

107. Razanskiene A, Schmidt J, Geldmacher A, Ritzi A, Niedrig M, et al. (2004) High yields of stable and highly pure nucleocapsid proteins of different hantaviruses can be generated in the yeast Saccharomyces cerevisiae. J Bitech 111: 319-333.

108. Emonet SF, Grard G, Brisbarre NM, Moureau GN, Temmam S, et al. (2007) Long PCR Product Sequencing (LoPPS): a shotgun-based approach to sequence long PCR products. Nat Protoc 2: 340-346.

109. Hall TA (1999) BioEdit: a user-friendly biological sequence alignment editor and analysis program for Windows 95/98/NT. Nucl Acids Symp Ser 41: 95-98.

110. Strimmer, K von Haeseler A (1997) Likelihood-mapping: a simple method to visualize phylogenetic content of a sequence alignment. Proc Natl Acad Sci U S A 94: 6815-6819.

111. Schmidt HA, Strimmer K, Vingron, M von Haeseler A (2002) TREE-PUZZLE□: maximum likelihood phylogenetic analysis using quartets and parallel computing. Bioinformatics 18: 502-504.

112. Tamura K, Peterson D, Peterson N, Stecher G, Nei M, et al. (2011) MEGA5: Molecular Evolutionary Genetics Analysis using Maximum Likelihood, Evolutionary Distance, and Maximum Parsimony Methods. Mol Biol Evol: In press.

113. Pfaffl MW (2001) A new mathematical model for relative quantification in real-time RT-PCR. Nucleic Acids Res 29: 2002-2007.

114. Pfaffl MW, Horgan GW, Dempfle L (2002) Relative expression software tool (REST) for group-wise comparison and statistical analysis of relative expression results in real-time PCR. Nucleic Acids Res 30: e36.

115. Radonic A, Thulke S, Mackay IM, Landt O, Siegert W, et al. (2004) Guideline to reference gene selection for quantitative real-time PCR. Biochem Biophys Res Commun 313: 856-862.

116. Kramski M, Meisel H, Klempa B, Krüger DH, Pauli G, et al. (2007) Detection and typing of human pathogenic hantaviruses by real-time reverse transcription-PCR and pyrosequencing. Clin Chem 53: 1899-1905.

117. Flohr F, Schneider-Schaulies S, Haller O, Kochs G (1999) The central interactive region of human MxA GTPase is involved in GTPase activation and interaction with viral target structures. FEBS Lett 463: 24-28.

118. Maes P, Klempa B, Clement J, Matthijnssens J, Gajdusek DC, et al. (2009) A proposal for new criteria for the classification of hantaviruses, based on S and M segment protein sequences. Infect Genet Evol 9: 813-820.

119. Martin DP, Lemey P, Lott M, Moulton V, Posada D, et al. (2010) RDP3: a flexible and fast computer program for analyzing recombination. Bioinformatics 26: 2462-2463.

120. Levine JR, Prescott J, Brown KS, Best SM, Ebihara H, et al. (2010) Antagonism of type I interferon responses by New World hantaviruses. J Virol 84: 11790-11801.

121. Yanase T, Kato T, Yamakawa M, Takayoshi K, Nakamura K, et al. (2006) Genetic characterization of Batai virus indicates a genomic reassortment between orthobunyaviruses in nature. Arch Virol 151: 2253-2260.

122. Briese T, Kapoor V, Lipkin WI (2007) Natural M-segment reassortment in Potosi and Main Drain viruses: implications for the evolution of orthobunyaviruses. Arch Virol 152: 2237-2247.

123. McElroy AK, Smith JM, Hooper JW, Schmaljohn CS (2004) Andes virus M genome segment is not sufficient to confer the virulence associated with Andes virus in Syrian hamsters. Virology 326: 130-139.

124. Rizvanov AA, Khaiboullina SF, St Jeor S (2004) Development of reassortant viruses between pathogenic hantavirus strains. Virology 327: 225-232.

125. Rodriguez LL, Owens JH, Peters CJ, Nichol ST (1998) Genetic reassortment among viruses causing hantavirus pulmonary syndrome. Virology 242: 99-106.

126. Coyne CB, Bergelson JM (2006) Virus-induced Abl and Fyn kinase signals permit coxsackievirus entry through epithelial tight junctions. Cell 124: 119-131.

127. Gale M, Katze MG (1998) Molecular mechanisms of interferon resistance mediated by viral-directed inhibition of PKR , the interferon-induced protein kinase. Science 78: 29-46.

128. Bergmann M, Garcia-Sastre A, Carnero E, Pehamberger H, Wolff K, et al. (2000) Influenza virus NS1 protein counteracts PKR-mediated inhibition of replication. J Virol 74: 6203-6206.

129. Dauber B, Martínez-Sobrido L, Schneider J, Hai R, Waibler Z, et al. (2009) Influenza B virus ribonucleoprotein is a potent activator of the antiviral kinase PKR. PLoS pathogens 5: e1000473.

130. Sharma K, Tripathi S, Ranjan P, Kumar P, Garten R, et al. (2011) Influenza A virus nucleoprotein exploits Hsp40 to inhibit PKR activation. PLoS One 6: e20215.

131. Matthys V, Gorbunova EE, Gavrilovskaya IN, Pepini T, Mackow ER (2011) The C-terminal 42 residues of the TULV Gn protein regulate interferon induction. J Virol 85: 4752-4760.

132. Hooper JW, Larsen T, Custer DM, Schmaljohn CS (2001) A lethal disease model for hantavirus pulmonary syndrome. Virology 289: 6-14.

133. Campen MJ, Milazzo ML, Fulhorst CF, Obot Akata CJ, Koster F (2006) Characterization of shock in a hamster model of hantavirus infection. Virology 356: 45-49.

Acknowledgements

I would like to express my great gratitude to Prof. Detlev H. Krüger, Director of the Institute of Virology, Charite Berlin, for giving me a chance to come to his laboratory and perform my PhD studies as well as for his motivation and support. I would like to thank my second supervisor Dr. Boris Klempa for fruitful discussions and valuable advices.

I appreciate Prof. Günther Schönrich and Dr. Thorsten Wolff for being members of my thesis committee, giving me excellent suggestions and navigating me through the performance of my PhD project.

My special thanks go to Dr. Andreas Rang, who helped me a lot in development and improvement of Western blot and real-time PCR techniques, for his readiness to discuss my thesis and to share his experience.

I would like to thank my lab-mates Brita Auste, Dr. Peter Witkowski, Dr. Sina Kirsanovs for helping me through difficulties in my experiments and for unlimited technical and personal support.

I would like to thank Dr. Jörg Hofmann and Dr. Jakob Ettinger from Diagnostics department of the Institute of Virology, Charite Berlin, for performing of serological studies of patient H431, for providing me with the sequences of this patient as well as for support and fruitful discussions.

As a participant of International ZIBI Graduate School, I would like to thank Prof. Richard Lucius, Dr. Martina Sick, Susanne Pocai, Dr. Susann Beetz for arranging multiple courses, seminars, retreats, student's days to get together all students of the program and for helping them to advance their skills and scientific knowledge. My PhD thesis would not be possible without financial support from Max-Planck Institute, DFG and Graduiertenkolleg 1121.

My special thanks go to my friends and students of ZIBI Graduate School Pritesh Lalwani and Dr. Chin-An Yang for setting up of many new techniques, for unlimited help in solving of all kind of problems, for sharing with me with their professional experience and scientific knowledge.

Finally, my great thank goes to my dearest parents, to my boyfriend Dima, to my best friends Tanya, Jenya, Lena for their endless trust in me, love, patience and support in all kind of situations happened during my stay abroad. I also want to thank the rest of my family, former Russian colleagues, university and international friends who helped me to reach this point in my life.

List of own publications

Popugaeva E., Witkowski P.T., Schlegel M., Ulrich R.G., Auste B., Rang A., Krüger D.H., and Klempa B. (2011) Greifswald virus, representative of Dobrava-Belgrade hantavirus causing hemorrhagic fever with renal syndrome in North-East Germany. *PloS One*, submitted

Klempa B., Witkowski P.T., Popugaeva E., Auste B., Koivogui L., Fichet-Calvet E., Meulen J., and Kruger D.H. (2011) Sangassou virus, the first hantavirus from Africa, displays distinct genetic and functional properties in the group of Murinae-associated hantaviruses. *J Virol,* in revision

Bulygin K.N., Popugaeva E.A., Repkova M.N., Meschaninova M.I., Graifer D.M., Ven'yaminova A.G., Frolova L.Yu. and Karpova G.G. (2007). C-domain of translation termination factor eRF1 neighbors stop codon at the 80S ribosomal A site. *Mol.Biol.*, Vol. 41, No. 5, pp. 858-67.
http://www.ncbi.nlm.nih.gov/pubmed/18240568?dopt=Abstract

Molotkov M.V., Graifer D.M., Popugaeva E.A., Bulygin K.N., Meschaninova M.I., Ven'yaminova A.G. and Karpova G.G. (2007). Protein S3 in the human 80S ribosome adjoins mRNA from 3'-side of the A-site codon. *Bioorgan. Chem.*, Vol. 33, No. 4, pp. 431-41. http://www.ncbi.nlm.nih.gov/pubmed/17886434?dopt=Abstract

Molotkov M.V., Graifer D.M., Popugaeva E.A., Bulygin K.N., Meschaninova M.I., Ven'yaminova A.G. and Karpova G.G. (2006). mRNA 3' of the A site bound codon is located close to protein S3 on the human 80S ribosome. *RNA Biol*, Vol. 3, No. 3, pp. 122-29. http://www.ncbi.nlm.nih.gov/pubmed/17179743?dopt=Abstract

Datum Unterschrift

Selbständigkeitserklärung

Hiermit erkläre ich, Elena Popugaeva, dass ich die vorliegende Doktorarbeit mit dem Thema: „Molecular characterization and pathogenicity potential of novel hantavirus isolates: Greifswald virus from Germany and Sangassou virus, Africa“ selbst verfasst und keine anderen als die angegebenen Quellen und Hilfsmittel verwendet habe.

Datum Unterschrift